Mafalda Dias de Medeiros Vale da Camara

Licenciatura em Ciências da Engenharia Biomédica

Coherence and Phase Locking Disruption in Electromyograms of Patients with Amyotrophic Lateral Sclerosis

Dissertação para obtenção do Grau de Mestre em
Engenharia Biomédica

Orientador : Hugo Gamboa, Professor Auxiliar, Faculdade de Ciências e Tecnologia da Universidade Nova de Lisboa

Co-orientadora : Carla Quintão, Professora Auxiliar, Faculdade de Ciências e Tecnologia da Universidade Nova de Lisboa

Júri:

Presidente: Doutor Mário Forjaz Secca

Arguente: Doutor Benjamim Ohana

Vogais: Doutor Hugo Gamboa
Doutora Carla Quintão

FACULDADE DE CIÊNCIAS E TECNOLOGIA
UNIVERSIDADE NOVA DE LISBOA

Novembro, 2013

Coherence and Phase Locking Disruption in Electromyograms of Patients with Amyotrophic Lateral Sclerosis

À minha família

Acknowledgements

First, I thank my supervisor, Professor Hugo Gamboa, who has challenged me throughout my thesis. I offer my sincerest gratitude to my co-supervisor, Professor Carla Quintão, who always presented me different paths and solutions when problems emerged, and encouraged me to think further; this work would have never been written without her support, motivation, knowledge, or patience. To Doctor Professor Mamede Carvalho and Doctor Susana Pinto, many thanks for allowing me the room and patients in Hospital Sta Maria, to perform acquisitions, and their availability and comfortable spirit. This thesis could not have been performed without their support, faith and trust in me. To both, I thank for the environment and knowledge that the Hospital offered me. To *PLUX-Wireless Biosignals*, S.A., professional workers for welcoming me every day and making me feel a part of the group.

To my colleges Marília and Inês, a big thank you to both for all the funny moments, adventures and help. A special thank you to Marília who stood by me every day with her available support, motivation and cheerfulness. Her daily presence made me win the day and without it, my work would have never been the same.

Por último mas mais importante, agradeço à minha família. Sem a sua paciência, motivação, crença e fé em mim, nunca teria chegado onde estou. Aos meus pais, um muito obrigado por tudo na vida e por serem os meus exemplos. Obrigada pelo constante apoio e por sempre aceitarem o caminho que escolho. Ao meu irmão pela constante preocupação que tem por mim. À minha avó e tios, por me fazerem sentir única e precisa. Ao Pedro Santana, um enorme obrigada pela atenção e paciência que sempre tem comigo, mas especialmente por me proporcionar os melhores fins de dia. Às amigas cuja companhia é uma necessidade, obrigada por me aturarem, ouvirem e motivarem. Obrigada pela diversão que fazem do meu dia. Tenho muito orgulho em todos e a vós dedico o meu trabalho.

Abstract

In motor neuron disease, the aim of therapy is to prevent or slow neuronal degeneration and early diagnosis is thus essential. Hypothesising that beta-band (15−30 Hz) is a measure of pathways integrity as shown in literature, coherence and PLF could be used as an electrophysiological indicator of upper and lower neuron integrity in patients with ALS. Before further analysis, synthetic EMG signals were computed to verify the used algorithm. Coherence and PLF analyses were performed for instants of steady contraction from contra and ipsilateral acquisitions. Ipsilateral acquisitions were performed for one member of each group and results present significant differences between both groups. Contrarily, contralateral acquisitions were performed on 6 members of each group and results present no significant differences. PLF analysis was computed for ipsilateral acquisitions and, similarly to coherence, results show significant differences between both groups. PLF was also analysed for contralateral acquisitions, and results show no significant differences within groups, as expected since no coherence was found for the same acquisitions. So, while control subjects present no neuronal or muscular problems and therefore higher synchrony and coherence for beta-band frequencies, patients with ALS do not present synchronism or coherence in any frequency, specially for beta-band. All results allowed to conclude that contralateral coherence is not a good measure of corticospinal pathways integrity. However, ipsilateral acquisitions show promising results and it is possible to affirm that ipsilateral measurements may reflect neuronal degeneration. For future work is suggested a deeper analysis of PLF, that appear to have potential as a quantitative test of upper and lower neuron integrity related to ALS.

Keywords: Contra and Ipsilateral, Coherence, Beta-Band, Phase Locking Factor (PLF), Amyotrophic Lateral Sclerosis (ALS), Electromyography (EMG).

Resumo

Em doenças neuromotoras, o objectivo da terapia é prevenir ou retardar a degeneração neuronal, sendo o diagnóstico precose essencial. Assumindo, como observado na literatura, que a banda beta ($15-30$ Hz) é uma medida de integridade dos percursos neuronais, a coerência e o PLF podem ser usados como um indicador electrofisiológico da integridade superior e inferior neuronal em pacientes com ELA. Para verificar o algoritmo utilizado foram criados sinais sintéticos de EMG. Análises de coerência e PLF foram realizadas para instantes de contracção estática em aquisições contra e ipsilaterais. Aquisições ipsilaterais foram realizadas num membro de cada grupo de sujeitos e os resultados apresentam diferenças significativas entre ambos os grupos. Pelo contrário, aquisições contralaterais foram realizadas em 6 membros de cada grupo e os resultados não apresentam diferenças significativas. Análises de PLF foram realizadas em aquisições ipsilaterais e, tal como na coerência, os resultados apresentam diferenças significativas entre ambos os grupos, enquanto que em aquisições contralaterais, os resultados não demonstram diferenças entre os grupos, uma vez que a coerência não foi significativa para estas mesmas aquisições. Enquanto sujeitos de controlo não apresentam qualquer problema neuronal ou muscular e portanto apresentam maior sincronia e coerência para a banda beta, pacientes com ELA não apresentam sincronismo nem coerência para nenhuma frequência, especialmente para a banda beta. Todos os resultados permitem concluir que coerência contralateral não é um bom indicador da integridade de percursos corticoespinhais. No entanto, aquisições ipsilaterias demonstram resultados promissores e é possível afirmar que podem reflectir degeneração neuronal. Futuramente sugere-se uma análise mais aprofundada do PLF, que aparenta ter potencial quantitativo no estado de integridade neuronal superior e inferior, relacionada com a ELA.

Palavras-chave: Contra e Ipsilateral, Coerência, Banda Beta, Phase Locking Factor (PLF), Esclerose Lateral Amiotrófica (ELA), Electromiografia (EMG).

Contents

List of Figures

Acronyms

ALS Amyotrophic lateral sclerosis

CNS Central nervous system

EEG Electroencephalography

EMG Electromyography

LMN Lower motor neuron

MEG Magnetoencephalography

MRI Magnetic resonance imaging

RMS Root mean square

sEMG Surface EMG

UMN Upper motor neuron

DC Direct current

NFFT Nonequispaced fast Fourier transform

FFT fast Fourier transform

PSD Power spectral density

CSD Cross power spectral density

PLF Phase locking factor

1

Introduction

1.1 Motivation

Amyotrophic lateral sclerosis (ALS), one of the major neurodegenerative diseases, is a progressive incurable motor neuron disorder fatal in all cases. Studies of European citizens established that the incidence of ALS is at 2 – 16 per 100 000 person-years. Despite being a global disease, incident data is still unknown. Associated therapy involves slowing down or even preventing neuronal degeneration, focussing on strategies for early diagnosis and/or treatment [2].

Significant efforts have been made to diagnose and cure this disease but research is focused on extending longevity, improving patients live quality and therapies, undertaking clinical trials, collecting population data in order to take measures to avoid onset and discovering triggers [2].

As a general rule, patients with ALS are diagnosed when there is already extensive motor neuron degeneration present, since the diagnosis is hampered by our impossibility to access the corticospinal tract. Since no definitive diagnostic test or biomarker exists for ALS but only clinical criteria, this project intends to measure coherence and Phase locking factor (PLF) between a number of specific muscles, establishing oscillation frequencies patterns in these patients.

1.2 Objectives

The aim of this thesis is to observe differences in frequency and time domains, between both control and patients with ALS group where upper motor neuron degeneration, associated with the difficulties in assessing corticospinal tract, is difficult to diagnose.

Based on Electromyography (EMG) signal patterns and behaviour, using coherence and PLF methods, the aim is to evaluate these patterns and determine whether an individual is affected by degenerative diseases. An acquisition protocol, signal recordings and processing are necessary in order to obtain information about physiological patterns enabling the comparison of different EMG signals in a given patient and later in a population with ALS.

1.3 State - of - the - art

As defined by El Escorial [3, 4], diagnosing ALS in patients requires electrophysiological tests (and the exclusion of other pathologies) to detect lower and upper motoneurons degeneration, being the last one the hardest to observe [5]. Much research has been conducted in order to provide faster and more accurate diagnosis for this disease. After El Escorial review, motor neuron disorders, where lower motor neuron abnormality is a primary feature, became a trustworthy diagnose [6].

To detect, evaluate and quantify upper or lower motor degeneration, some methods have been used, that may also be used as possible progression markers for clinical trials, such as nasal pressure, maximum voluntary isometric contraction, neurophysiological index, motor unit estimation, transcranial magnetic stimulation, magnetic stimulation, triple stimulation technique, needle EMG signal analysis, tractography and diffusion tensor-weighted Magnetic resonance imaging (MRI) [7, 5, 8]. These methods either detect upper (less often) or lower motor neuron degeneration and usually with undetermined sensitivity, extremely high costs and pain to the patient. Concerning therapy, Riluzole (a drug), has been used in early trials with promising results [6].

Diagnosing motor neuron disease has been chiefly hampered by the incapacity to observe corticospinal tract integrity [6]. In order to evaluate corticospinal damage, Babinskisign and hyperreflexia may be useful as markers but they were proven not to be exclusively indicators of such damage. As an alternative method to assess upper motor neuron

integrity, propagation of oscillatory activity may be studied. *Farmer et al.* [9] showed that during movement development, both in frequency and time domains, synergetic action of separated muscles becomes more closely connected by an increase in shared synaptic drive. As shown in [9], EMG – EMG coherence analysis reflects oscillatory synchronization between common inputs to spinal motoneurons in specific frequency values and originates from synchronous oscillations within networks of corticospinal neurons that are then transmitted to spinal motoneurones via fast-conducting corticospinal pathways. In *Farmer et al.* [9] has also been demonstrated that in the beta frequency (one type of motor cortical oscillation) coherence and motor unit synchrony are present, pointing to a significant common drive that leads to coactivation of muscles closely related and hypothesized that it is associated with more efficient motor unit recruitment and increased speed and accuracy when performing a motor task. Equally, *Baker et al.* [10] postulated that these beta frequency oscillations provide a more efficient motor unit recruitment than that provided by non-oscillatory drive. As defended in *Fisher et al.* [6] in normal subjects, beta-band oscillations can be observed in intermuscular coherence between different muscles, proving a common cortical drive, and dependent on supraspinal structures. Motor cortical oscillations are coherent with those in contralateral electromyograms as observed in *Baker et al.* [11]. Also in *Baker et al.* [11] it was proven that coherence between EMG and afferent discharges exists at higher frequencies, during a step-hold isometric task.

Different frequencies seem to be related to the timing of different neuronal assemblies (activated parts of network) which are associated with different types of sensory and cognitive processes [12].

Some motor cortex cells are capable of synchronizing their discharge with local oscillations in a 20 – 30 Hz range of frequency. This synchronism happens during rest or steady contraction but is not common during movement. Despite all the research on this subject, there is no agreement on which function might induce such periodic activity [11]. Recent studies showed that corticomuscular coherence may be induced by ascendant and descendent pathways, suggesting synchronous oscillations in sensorimotor processing instead of playing a purely motor role [6]. Some oscillatory cortical activity involves pyramidal neurones and is reflected in the descending drive to the muscles, being distributed to agonist and antagonist muscles, which can be observed in the EMG of these

muscle pairs through coherence in beta-band [13]. In *Cordivari et al.* [13] the authors conclude that EMG - EMG coherence may be observed and modulated by peripheral nerve stimulation. Motor unit recruitment and firing rate are essential to perform voluntary movement and for motor control [8]. *Mamede de Carvalho et al.* [8] analysed firing rates of motor units during slight voluntary activation in patients with ALS and compared them with normal subjects in order to establish firing unit patterns and concluded that in ALS patients firing rate within lower motor neurons decreased comparatively to normal subjects, thus diagnosis lower motor neuron degeneration.

Short duration synchronization has been established between pairs of motor-unit spikes during the performance of a task in intrinsic hand muscles by observing a central peak in cross-correlation histogram. In *Conway et al.* [14] the authors suggest that this synchronization between motor units originates in rhythmic activity in central motor pathways that provide common inputs to motoneuronal pairs. Also in *Conway et al.* [14], using Magnetoencephalography (MEG), it's exposed the relation between localized rhythmic cortical activity and motor-unit activity. In several studies, as suggest in *Mima et al.* [15], it is now accepted that synchronization between two separate neural systems reflects the functional coupling between them.

Coherence and cross-correlation analyses have been applied to human walking activity and it was demonstrated that motor units from synergetic muscles receive a common synaptic drive that is adjustable during task cycle and depends on an intact supraspinal drive to the spinal cord [16]. Corticomuscular coherence measures contributions from both ascending and descending pathways, which was proved by phase analysis, suggest that muscles led the cortical recordings [17]. The timing of synchronism is dependent on the intrinsic properties of the inhibitory interneurons and their conduction delay [18]. In *Riddle et al.* [19] it was found that corticomuscular coherence does not behave uniformly between subjects and a plausible explanation may be the differences of multiple interacting oscillatory processes, each of them with underlying phase relationships. Moreover, evidence was obtained showing that coherence is a complex composite of multiple interacting processes probably with a contribution from both afferent and efferent systems.

In order to diagnose disorders such as ALS, it is necessary to observe upper and lower motor neuron function. Many techniques, as shown above, can be used to study it in various processes, which are either invasive, inaccurate or only allow diagnoses of

either upper or lower degeneration (not both). This thesis intends to present a new non-invasively form of studying upper and lower motor neuron degeneration, in the context of *Fisher et al.* [6] publication, based on coherence and PLF intermuscular analysis and providing a new effectively early diagnose of ALS.

1.4 Thesis Overview

This work structure can be divided in different steps represented in figure 1.1. The first two chapters are based on literature review related to signals analysis and ALS characteristics. Throughout this stage, state-of-the-art and theoretical background about EMG signal, ALS, neuronal behaviour and time and frequency domain analysis, is reported and documented. In response to the absence of a precise and quantitative method of diagnosing ALS, coherence and PLF analyses were performed. Chapter 3 discusses the acquisition protocol, groups of subjects and recording. Chapter 4 refers to signals processing, namely to low and high level, including coherence and PLF algorithm analysis. Chapter 5 discusses all obtained results in this work, through algorithm validation tests, coherence and PLF results from ipsi and contralateral acquisitions. Chapter 6 presents all conclusions from the entire work. Appendix contains two published papers within the context of this research work. The language used to write this thesis was LATEX and the software used to analyse all acquisitions was Python.

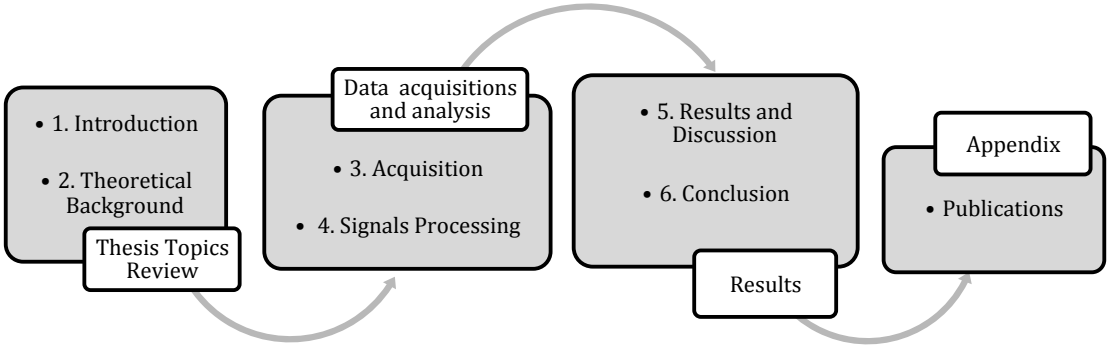

Figure 1.1: Thesis Overview Diagram.

2

Theoretical background

This chapter, through different stages, contextualizes all aboard subjects in this work.

2.1 Scientific support

2.1.1 ASL – Amyotrophic Lateral Sclerosis

ALS is one of the major neurodegenerative diseases, a progressive disorder that involves widespread degeneration of the motor system neurons from the destruction of layer V pyramidal neurons from the motor cortex to the anterior horn of the spinal cord. It is a devastating pathology with rapid and aggressive progression, with uncertain pathogenesis and fatal in outcome, with 50% of patients dying within 3 years of onset [6, 7]. To diagnose such disease it is necessary to find upper and lower motor neuron degeneration in multiple regions: bulbar, cervical, thoracic and lumbar. Some features can be useful as prognosis indicators, such as increased age of onset, low forced vital capacity, bulbar onset and short time duration between the first symptoms and its presentation [7].

This disorder is characterized depending on the neurological regions affected, but there are common features observed in all patients such as a rapidly progressive weakness, muscle atrophy, muscle cramps, fasciculations, muscle spasticity, difficulties in breathing – dysponea, difficulties in swallowing – dysphagia and difficulties in speaking –

dysarthria. Patients tend to lose their abilities to control voluntary movements and symptoms tend to greatly reduce their quality of life [2].

Many causal and pathogenetic hypotheses have been studied and proposed but the disease remains poorly understood in terms of unifying causal hypothesis. Some factors may alter the risk of developing ALS such as environmental factors, toxic risks factors, family history, smoking, life-style, neurotoxins, consanguinity and genetic mutations with the copper/zinc superoxide dismutase (SOD1) being the major one [7, 2]. Recent studies focused on glutamate-induced excitotoxicity, dysregulation of intracell calcium, autophagy, structural abnormalities of mitochondria, dysfunction of the sodium/potassium ion pump, axonal transport defects and protein aggregation as other additional pathologenic hypotheses [7, 2]. The mechanisms that mediate motor neuron degeneration by glutamate-induced excitotoxicity are supported by "dying - forward", "dying – back" hypothesis, or even that lower and upper degeneration occurs independently. Evidence and explanations for all theories can be found in [2] and are showed in figure 2.1.

So far, only riluzole – an inhibitor of glutamate neurotransmitter - has been licensed as a disease-modifying strategy for ALS, which is used to extend the lifespan of these patients by 3 months, but some others have been investigated: nerve growth factor, recombinant insulin-like nerve growth factor 1, ciliary neurotrophic factor and brain-derived neurotrophic factor [7]. Since this disorder is incurable so far, patients are administered with drugs that can relieve some symptoms and help cope with pain, particularly musculoskeletal pain.

2.1.2 Propagation of nervous impulses

Central nervous system (CNS) influences muscle activity through two sets of neurons: Upper motor neuron (UMN) and Lower motor neuron (LMN). A schematic representation is shown in figure 2.2.

Upper motor neurons are derived from the motor cortex or the brainstem and carry information through descending pathways until a specific nerve root from the spinal cord, and are responsible for driving impulses for voluntary motor activity. The lower motor neuron brings information from UMN to muscle fibres. They can be classified according to the muscle fibre type they innervate: alpha motor neurons which innervate extrafusal muscle fibres and are responsible for muscle contraction, and gamma motor

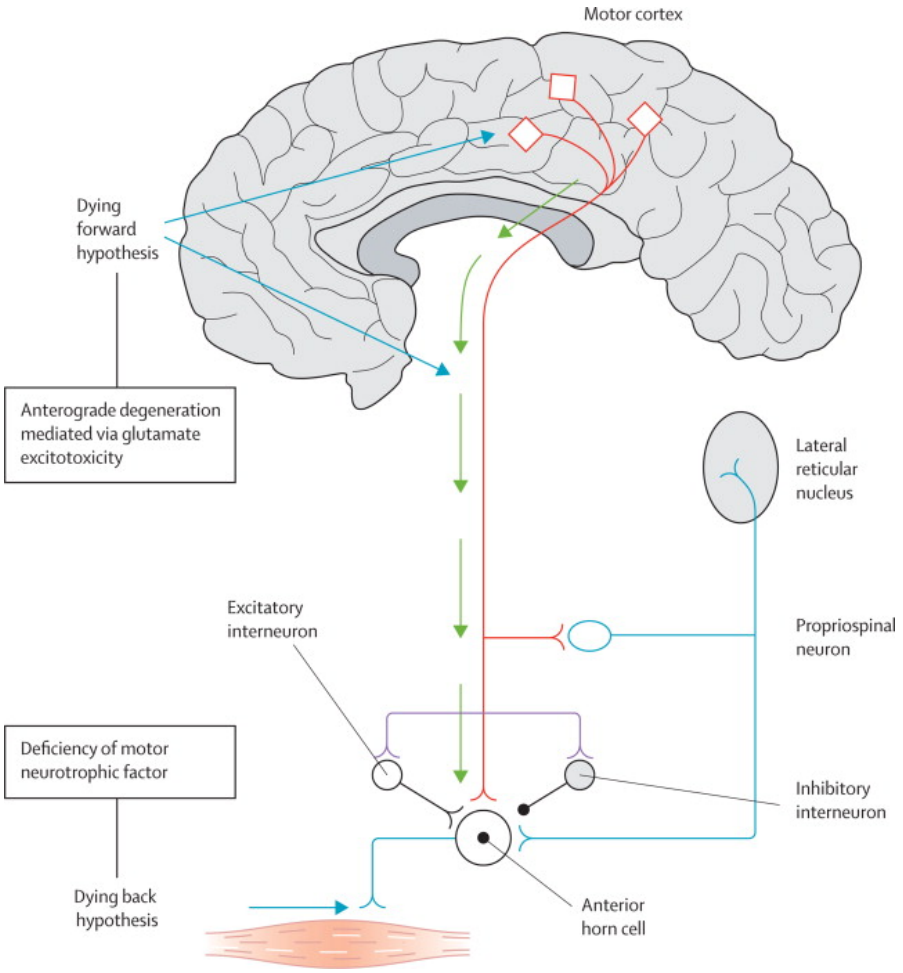

Figure 2.1: Dying – forward" postulates that ALS is a disorder of corticomotoneurons, which connect monosynaptically with the anterior horn cells, mediating anterograde degeneration of anterior horn cells (via glutamate excitotoxicty). The "dying – back" theory postulates that ALS begins within muscle cells or neuromuscular junctions; there is a deficiency of a motor neurotrophic hormone, which is normally released by postsynaptic cells and retrogradely transported up the presynaptic axon to the cell body.

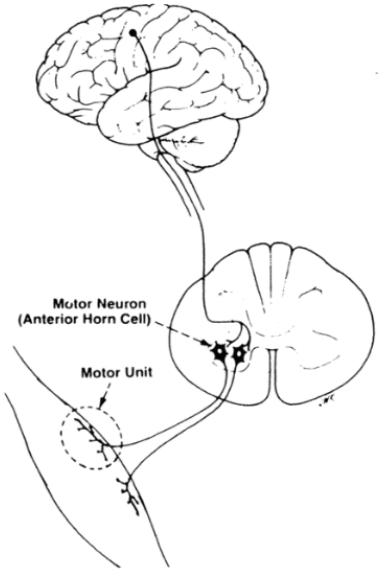

Figure 2.2: Upper motor neurons driving impulses through descending pathways into spinal cord – anterior horn cell - nerve root, which via synapses (glutamate neurotransmissor), transmit information to lower motor neurons, which via synapses (acetylcholine), transmit it to muscle fibres.

neurons which innervate intrafusal muscle fibres and are responsible for proprioception. All voluntary movements and motor control depends on motor unit recruitment and firing rate, and hence the arousal of LMN by UMN, by means of synapses. As demonstrated in the first study of motor unit activation performed with normal subjects (Adrain and Bron, adapted from [20]): force exerted by a muscle during a voluntary contraction was the result of the concurrent recruitment of motor units and modulation of the rate at which they discharged action potentials.

2.1.3 Motor units and action potentials

Motor units are the basic component of muscular strength and contraction. Motor units are composed by a motor neuron with a variable number of branches – depending on muscle specificity - ending in different muscular fibres of the same type, innervated by the motoneuron [1]; Schematic representation is shown in figure 2.3.

To initiate the generation of muscle contraction, the CNS sends an electrical signal to a motoneuron, which spreads along muscle fibres, initiating a cascade of electrophysiological and electrochemical processes, giving rise to de-polarization and re-polarization events known as action potential or nervous impulse that can be electrically measurable. Transmitting information via the nervous system is based on the propagation of action

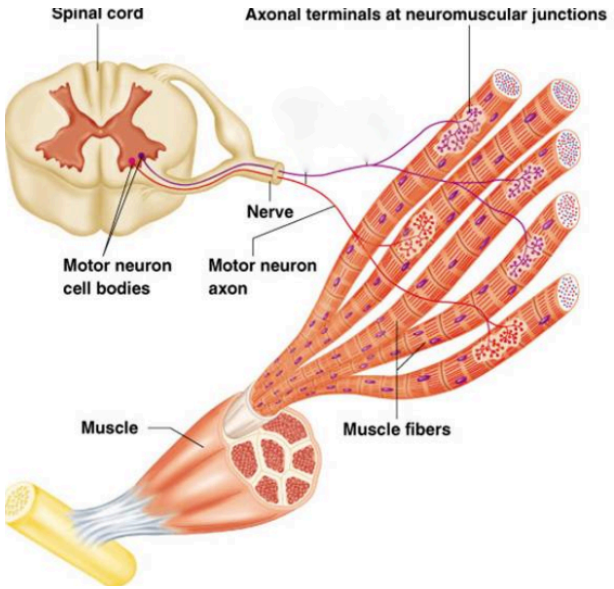

Figure 2.3: Schematic representation of a motor unit, composed by a motoneuron from the spinal cord, innervating muscle fibres through neuromuscular junction [1].

potentials along a nervous fibre, by means of diffusion and the intensity of muscle contraction is controlled by the regularity of action potentials, i.e., how often it arrives and innervates muscle fibres [1]. When a motoneuron receives an excitable signal, an action potential reaches muscles fibres innervated by it through one terminal branch of the axon– 'one-to-one' relationship [1]. In response to a single stimulus, one single action potential provokes a twitch contraction during 25 to 75 ms, as shown in figure 2.4.

When multiples stimulus are delivered to muscle fibres before their relaxation, the evoked force can be greater than a single impulse due to a mechanical summation (leading to a sustained contraction also known as tetanus), meaning that the response of muscle fibre is independent of the stimulus amplitude but proportionally dependent on the frequency of multiple stimulus, i.e., increasing frequency stimulus increases the muscle force produced. The CNS controlling the number of recruited motor units or their firing rate, between 8Hz to 35Hz, determines the force of muscle contraction [1].

2.1.4 Electromyography (EMG)

EMG is a technique that monitors electric activity of excitable cell membranes, based on the linear propagation of action potentials along muscle fibres. Electromyogram signal is the algebraic sum of all the detected signals within a certain area – representing voltage as a function of time - and may be affected by muscular, physiological, anatomic properties, peripheral nervous system and instrumentation used to acquire the signal [21].

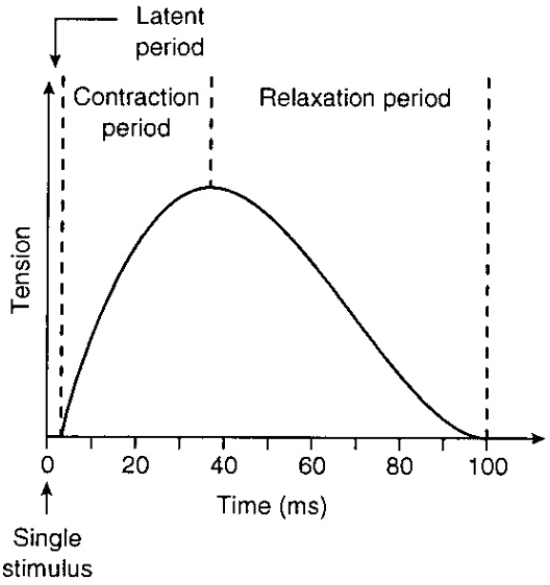

Figure 2.4: Schematic representation of twitch contraction as a response to a single stimulus after a latent period.

EMG is an important method to analyse muscular functioning, expressing in real time, muscular activation during movement, its activation intensity, duration and variability [21]. EMG signals can be acquired by surface electrodes attached to the skin over the target muscle – interferential process – or by needle electrodes inserted invasively into the muscles tissues – intramuscular process. Surface EMG (sEMG) measures action potentials along the entire recorded area underneath the electrodes, while needle electrodes measure action potentials from a small number of fibres and may not be representative of the entire muscle mass involved [1, 22]. sEMG appears to be more practical but it is easily contaminated by volume conduction between muscles. Intramuscular needle recording is more useful when using multi-motor units rather than single unit, since it provides more specific information - better signal-to-noise-ratio.

In this work, sEMG is used in order to estimate the number of activated motor units and their discharge rate on superficial muscles [22]. sEMG is more frequently used since it is a non-invasive procedure, painless and risk-free for the patient whose signal is being required, does not require specialized medical doctors and is more directly correlated with the mechanical outcome [22]. Two electrodes are placed on the skin over the muscle region to be analysed and the difference of potential between them is acquired and amplified [1].

The quality from EMG signals can be measured through signal-to-noise ratio, where

quality is higher when the ratio is greater and also from a common mode rejection ratio, that eliminates through differentiation common interferences (from electric networks, distance from muscles or heart beating) that are considered as noise during EMG recordings.

2.1.5 Patterns in EMG analysis

Voluntary movement is associated with the presence of rhythmic activity in motor cortex. Beta-band, comprising a range of frequencies from 15 to 30 Hz, appears to vary its magnitude prior and during voluntary movements and is associated with the attempt to perform certain tasks [23]. In this same frequency band, cortical activity and motor unit firing are correlated during sustained voluntary contractions. Intermuscular correlation (EMG - EMG) between different muscle groups appears to detect characteristics of the same rhythmic processes suggesting a common drive from corticospinal pathways. The precise function and genesis of these same cortical oscillations still remains elusive [24].

Firing rates of motor units are modulated by an 8 -12 Hz rhythm. Motor units from muscle pairs can be modulated by a descending 15 -30 Hz drive, demonstrating that this drive is mediated via corticospinal pathways (corticospinal cell activity encodes motor cortical oscillations), that oscillations within this band occur in the sensorimotor cortex which are coherent with contralateral muscles [24, 25]. These oscillations may arise in motor systems in order to promote synchronous neuronal firing between neurons populations that are spatially distributed but functionally related, providing means of linking different neuronal populations [24]. Coherent activity may represent a common element in coding activity in simultaneous active motor centres.

Cortical areas involved in the same motor task may be coherent with each other. Active muscles show coherence around beta-band, reflecting the activity of neuronal structures involved in driving the spinal motoneurons [25]. Coherence has demonstrated that some of these oscillations are probably transmitted via the pyramidal tract to activate muscles and may induce the same rhythm among them [25].

2.2 Technical base

2.2.1 Signal Acquisition

The signal acquisition process initiates with the placement of pairs of electrodes at varying distances along the muscles to compute coherence and PLF analysis between pairs of muscles, while subjects perform a specific task [16]. For the same performed task, data is collected by ipsilateral (electrodes situated on the same side of the body) and contralateral (electrodes situated on opposite sides of the body) acquisitions. In ipsilateral acquisitions, data is collected from the first dorsal interosseus and extensor digitorum communis muscles. In contralateral acquisitions data is collected from first dorsal interosseus muscles from each side of the body.

2.2.2 Recording device

EMG signal is recorded using bioPLUXresearch unit, shown in figure 2.5. This device collects real time biosignals and transmits them via bluetooth to a computer or smartphone, where they can be saved and visualized. BioPLUXresearch has eight analog sample channels with 12-bit of resolution, a sampling frequency of 5 KHZ and EMG sensors with second order band pass filter with cutoff frequencies of 25 and 450 Hz. The unit has also an external channel to be used as reference ground electrode for electrophysiology measures and a digital port for applications that require external synchronism.

2.2.3 Sampling frequency

Sampling frequency is of utmost importance to correctly acquire EMG digital signal and therefore, according to Nyqüist Theorem, at least the double of the highest frequency in EMG signal should be used as the sampling frequency. sEMG may have frequencies of up to 500 Hz – these values are affected by motor unit and contraction, electrodes sizes and distance between them – and the minimum sampling rate value should be 1 KHz [21, 26].

Figure 2.5: BioPLUXresearch system.

2.2.4 Electrodes

Electrodes are sensors of input and output of electric current that must be placed, in sEMG, near the muscle associated with a conducting gel that promotes a stable transmission as a function of time with low noise, in an electrode-tissue interface named superficial detection, so as to capture its ionic current that behaves as a low-pass filter [26, 21]. EMG signals are recorded with a bipolar configuration that consists of a combination of signals derived from two electrodes. The main advantage of such a configuration is that benefits from a high rate of common rejection and being the detection differential, potentially masked with high noise from power lines and the resulting signal, can be subtracted from both signals recorded in two different sites that is subsequently amplified – which means that any noise or artefact common to both signals is eliminated and the uncommon parts become amplified [21]. The placement of electrodes is crucial since muscles are composed by different types of muscle fibres – slow and fast twitching fibres – and therefore the amplitude of EMG and power spectral density are greatly variable. It is advised to place the electrodes in the proper location onto the muscle to avoid contamination by a neighbouring muscle's electrical activity, a phenomenon known as cross-talk (recommendations for electrode placement can be found in [26]); if the electrodes are

placed too close to each other, no difference of potential is detected, but greater distance causes more filtering [1].

2.2.5 Low-level processing

The EMG signal acquired is an analogue signal – continuous in time – that must be converted into a digital signal – discrete, defined by established intervals – so that can be digitalized to the computer [21]. Some parameters have to be analysed in frequency and time domains (as shown in subsections 2.2.5.1 and 2.2.5.2), that may be useful to better understand signal content for the aim of this project.

2.2.5.1 Time domain

Such analysis is based on the information of the amplitude of an EMG signal as a function of time, where amplitude represents the magnitude of muscular activity determined by motor units activity and their firing rates [21].

- **Rectification**

  Rectification consists on the transformation of EMG signals into their absolute values and it can remove its negative phases (full wave) or remove its negative values from the EMG raw signal. Rectification is applied in all signals prior to coherence analysis, since it exposes the contribution of low frequencies produced by action potentials.

- **Filters**

  Filters are used to attenuate a specific range of frequencies that are undesired and allow the passage of unaltered frequencies. Filters can be classified according to the specific range of frequencies that are attenuated and to choose the appropriate, one must priorly know which frequencies wants to work with. On this present work, for all signals are applied a band pass filter defined by cutoff frequencies Fc1 and Fc2, where all frequencies above Fc1 and bellow Fc2 are attenuated to zero. To describe filters behaviour, transition band is characterized by its order.

2.2.5.2 Frequency domain

Frequency is analysed since it is variable and dependent on firing rates from motor units, time of firing rates between different motor units and the shape of the action potential, the

latter having the greatest impact [21]. All real continuous signals can be represented by a combination of multiple sinus and cosinus, making use of fast Fourier transform (FFT) and construct a Power spectral density (PSD) which represents the signal strength as a function of frequency.

- **Frequency Spectra**

  Frequencies spectra allow to, through FFT analysis, observe frequency intensity. The spectrum of a signal is a positive real function of a frequency variable associated with a stationary stochastic process, with dimensions of power or energy per hertz (Hz). The spectrum decomposes the content of a stochastic process into different frequencies present in that signal, and helps identifying periodicities.

2.2.6 High-level processing

In adults, analysis of EMG rectified signals and motor unit firing between different co-contracting muscles show coherence at frequencies in a range of 1 - 45 Hz, with a higher frequency range in 16 – 32 Hz and a maximum in a lower frequency range in 1 -12 Hz [9]. Since it is known that cortical signal recorded in primary motor cortex interacts with muscle signal in specific frequencies, EMG - EMG coherence analysis detects oscillatory drive from corticospinal pathways and EMG is coherent with sensorimotor cortex Electroencephalography (EEG) and MEG, it is of interest to detect differences in EMG coherence in patients presenting ALS [9].

This evaluation is based on changes in occurrence and strength of EMG - EMG pairing as function of frequency and time – coherence and PLF estimates. PLF and coherence analysis of motor unit firing behaviour can provide information about the organization of networks responsible for driving spinal motoneurons during task performance and assess common presynaptic inputs that synchronize motor units populations [16]. In the human body, different activities may be characterized by functional activities in distinct circuits, due to muscles discharges at a certain frequency by CNS. Some of these oscillating frequencies led to spinal motoneurones and its results and origins can be found in [27].

2.2.6.1 Coherence

Rectification of sEMG is known to maximize the information regarding timing motor unit potentials. Rectified y and x are assumed to be realizations of stationary mean time series. Using discrete Fourier transforms, in frequency domain auto spectra $f_{x,x}(\lambda)$, $f_{y,y}(\lambda)$ and cross spectrum $f_{x,y}(\lambda)$ are calculated to assess measures of correlation [9, 28]. As a function of frequency, coherence $|R_{x,y}(\lambda)|^2$ is assessed by the squared magnitude of the normalized cross spectrum, divided by the product of the two auto spectra as show in equation 2.1.

$$|R_{x,y}(\lambda)|^2 = \frac{|f_{x,y}(\lambda)|^2}{f_{x,x}(\lambda) f_{y,y}(\lambda)} \tag{2.1}$$

Coherence function provides an output assuming values from 0 to 1, assuming value 0 if they are not linearly dependent on each other at any frequency and 1 when signals present a perfect linear relation between them. Thus, coherence provides a measurable quantity of the fraction of the activity in one sEMG signal that can be foreseen by the activity of the other sEMG signal [28, 9]. Hence, coherence quantifies the intensity and range of frequencies where rhythmic synaptic inputs are common across the motoneuron pool [16]. It should be pointed out that coherence does not provide the direction of interaction between both signals, only direct coherence, which won't be calculated since it has no relevance in this work.

2.2.6.2 PLF - Phase Locking Factor

During oscillatory activity, neurons fire synchronously. Therefore, common target cells will receive neural activity synchronously and so, oscillations play an important role for the timing of neural activity [12]. Synchrony plays an important role when performing a motor task, involving oscillating processes. On the assumption that coherence exists for the beta-band between two signals, for these frequencies both signals must be synchronized within each other. Many methods allow the observation of synchrony behaviour but PLF is the one used on this work. To obtain meaningful phase values, it is necessary the presence of oscillations in time series signals. Therefore, a transformation is needed to project the time series onto a circumference and extract the angle of rotation over time.

Presence of oscillatory activity may be observed prior to phase analysis by performing power spectra. After finding the frequencies peaks of interest (in this case beta-band),

they are isolated by applying to the signal a band-pass filter at a narrow band centred at each frequency of interest. From the obtained oscillatory signal, the angle of rotation, or phase, can be defined in the complex unit circle for each data point. The method used is based on the Hilbert transforms of the data. The only essential requirement for this method is that the signals contain a clear oscillatory component. An essential parameter in this analysis is the number of oscillation cycles considered. Longer observation times return more reliable estimates and too short observation periods may conceal important interactions, when they are weak or hidden by noise [29]. For signals j and k, $\phi_j(t)$ and $\phi_k(t)$ represent signals phase dependency on time, respectively, for $t = 1, ..., T$. PLF between both signals is defined by [30]:

$$\rho_{jk} \equiv |\frac{1}{T}\sum_{t=1}^{T} e^{i[\phi_j(t)-\phi_k(t)]}| = |\langle e^{i[\phi_j(t)-\phi_k(t)]}\rangle| \tag{2.2}$$

PLF assumes values from 0 to 1. 0 stands for signals entirely asynchronous, with phases randomly distributed, for T sufficiently long; 1 stands for signals perfectly synchronized and their phase lag constant. Values between 0 and 1 represent partial synchrony. PLF on this work is only calculated between two signals, specifically for all instants of steady contraction, where oscillations are expected. As assumed in literature, [29], lost of timing information caused by filtering is acceptable. Cutoff frequencies for the band-pass filter are chosen under the assumption that a particular frequency band shows the relevant information. Since beta-band is being analysed and comprehends a sufficient large interval, for each contraction PLF is performed as many times as the number of frequency values from the band.

To compare results between different subjects, estimates of pooled coherence and PLF are calculated to provide a single measure that summarizes all data across several subjects. Pooled estimates have the same type of outputs than coherence and PLF but refer to an entire population. This analysis of coherence and PLF provides mean values for a given muscle pair in single subjects, allowing the estimation of the probability distribution of mean beta-band coherence and PLF within a population.

3

Acquisition

In this chapter, different sections explain all collected data from the groups of subjects, recording system, experimental setup and the acquisition protocol.

3.1 Subjects

Focussing on previously published results, ipsilateral measurements were performed on 1 member from the group of patients and 1 member from the group of control. Contralateral measurements required the existence of two different groups of subjects: group of 6 patients presenting ALS and a control group of 6 subjects. All participants from the control group do not present any known neuronal or muscular disease, whereas patients with ALS have been diagnosed within less than 1 year. Acquisitions were performed in more patients but were not taken into account since these patients with ALS were in a more advanced stage of the disease, presenting motor difficulties that limited there own movement control, making impossible to collect an analysable EMG signal. In figure 3.1 is represented the ability (3.1(b)) and inability (3.1(a)) of self controlled movements in patients with ALS depending on this disease progress.

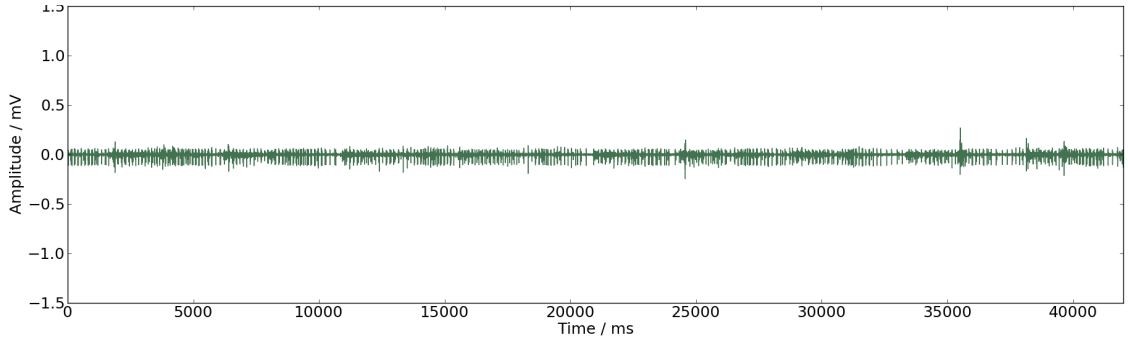

(a)

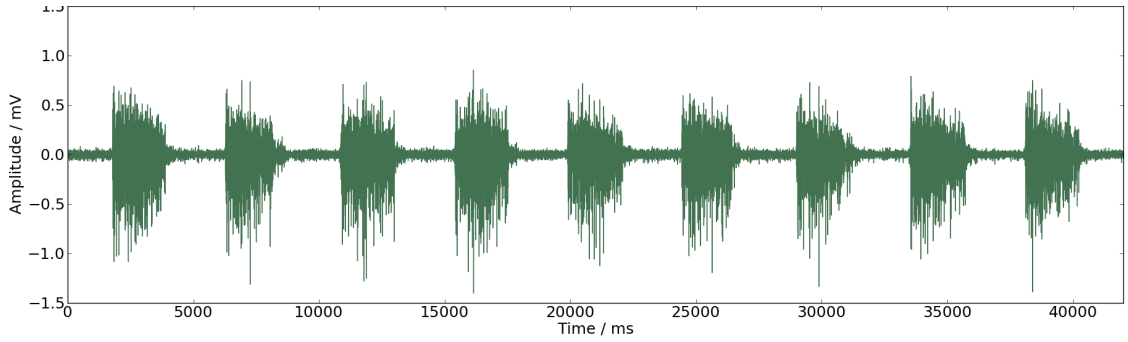

(b)

Figure 3.1: (a) EMG signal from a patient with incapacity to control his own movements. (b) EMG signal from a patient with capacity to control his own movements.

3.2 Acquisition Protocol

The performed task was the same used for ipsi and contralateral acquisitions. Subjects were asked to seat and place both hands on a desk, 10 cm away from each other in a parallel position and with hand palms facing each other, in 90 degrees of flexion with the elbow. Subjects had to elevate both index fingers vertically with a maximum articular amplitude in a direction opposite to the other fingers position, hold that position for 3 seconds while maintaining a certain force/pressure and then return to the initial position, where it remains for 3 seconds while relaxing as much as possible. This movement was repeated for 5 minutes or less according to maximum time tolerated by the patients. The coordinated movement was guided by a programmed sound and both fingers had to be as much coordinated as possible one to another.

3.3 Recording

For each ipsilateral acquisition, 4 signals were simultaneously acquired from each subject using EMG sensors attached to a bioPlux device. As observed in figure 3.2, besides the contralateral acquisition (as shown in figure 3.3), ipsilateral was simultaneously acquired. For both right and left hand, signals were collected using two sensors attached to first dorsal interosseus muscle; for both right and left forearm, signals were collected using two sensors attached to extensor digitorum communis muscle. Ground was placed in ulna bone inferior extremity, where no muscle activity is present.

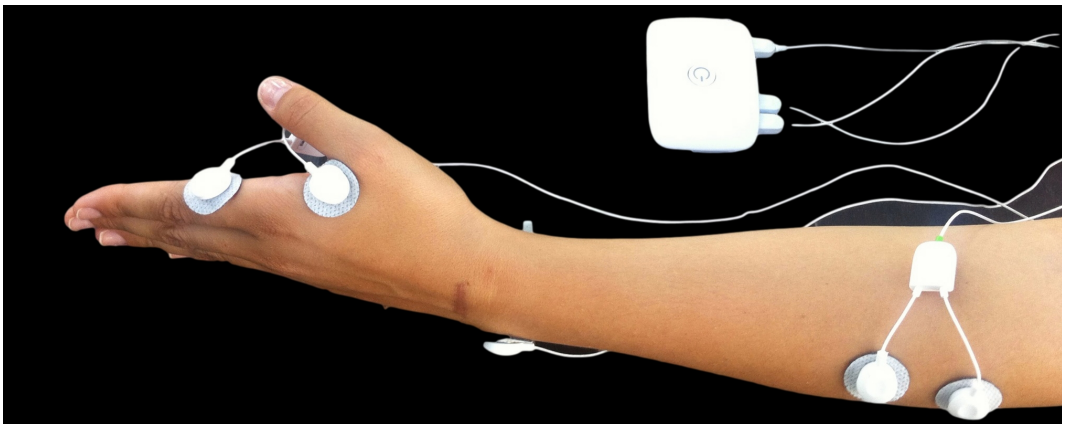

(a)

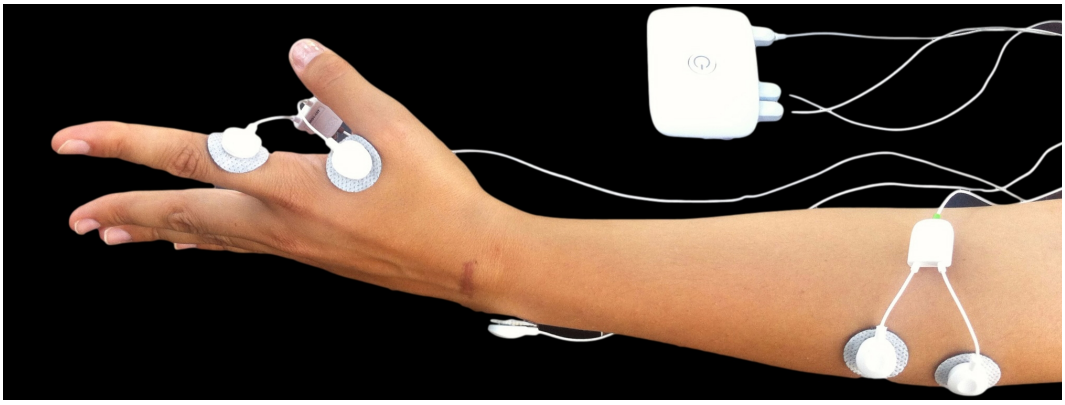

(b)

Figure 3.2: Ipsilateral acquisitions experimental setup: Bioplux research device, placement of two EMG sensors and ground. (a) Instant of relaxation. (b) Instant of contraction.

For each contralateral measurement, two signals were simultaneously acquired from each subject using two EMG sensors attached to a bioPlux device. Each sensor (one

for each hand) has two connected electrodes placed in first dorsal interosseus muscle. Ground was placed as in ipsilateral recordings. Surface electrodes placements are shown in figure 3.3. The device used and its specifications are explained in chapter 2.2.2.

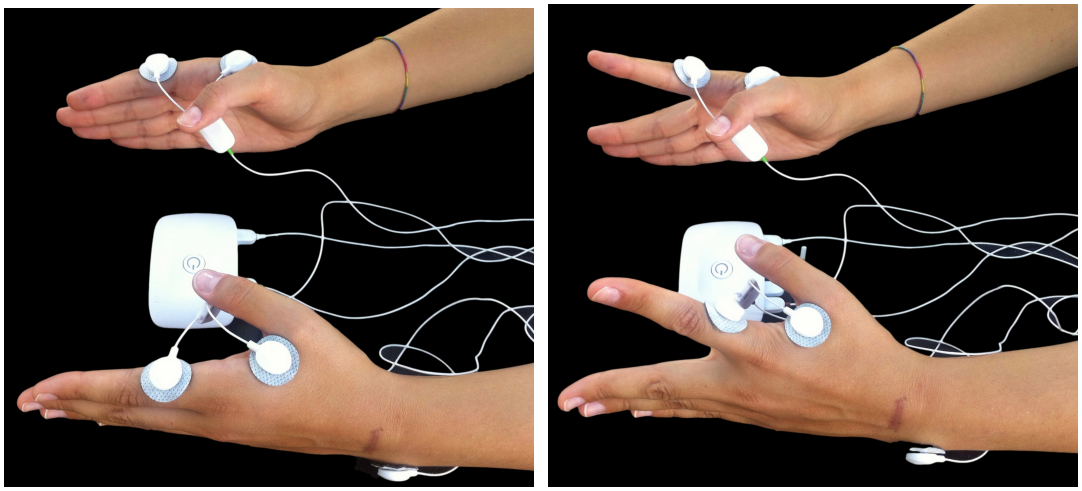

Figure 3.3: Contralateral acquisitions experimental setup: Bioplux research device, placement of two EMG sensors and ground. (a) Instant of relaxation. (b) Instant of contraction.

4

Signals Processing

This chapter discusses the algorithm and processing applied to all of the acquired data. Low level processing gathers instants of contraction so that high level processing calculates coherence and PLF mean values averaged for all subjects. This procedure allows to study ipsi and contralateral coherence and PLF for the beta-band frequency.

4.1 Low-level Processing

Both acquired signals were processed using Python language. Signals amplitude was changed from 'bins' into 'mV'. Signals were then filtered by a third order *butter* band pass filter of 30 – 2000 Hz (filter is shown in figure 4.2(a)); from these filtered signals, its envelope was calculated and its Direct current (DC) component removed. In order to extract information about coherence, intervals of contraction common to both signals had to be isolated from intervals of relaxation, since coherence is better estimated during periods of steady contraction [6]. Signals presenting higher amount of noise will conceal real information, inhibiting to distinguished contractions from relaxation intervals so predictably. This and the differences among individuals signals, does not allow to predefine an onset value common to all signals. So, instead of using a method based on the EMG signal envelope, a method based on statistical model was used. To determine the moments of muscular activations, an onset value had to be defined, through a method

that divides data in two different Gaussian distributions, one corresponding to the noise component of the original signal and the other to signal's relevant information. The onset value is defined by the covariance value derived from the noise Gaussian distribution, and multiplying it by a constant - previously achieved by experimental verification and dependent on each analysed data.

The signals acquired from patients and posteriorly ignored (referred in chapter 3.1) correspond to patients presenting difficulties in moving both fingers co-ordinately and maintaining a certain force value during contraction. Therefore, for these patients distinction between moments of muscular activation and the rest of the signal was not analysable.

For both signals, a vector was created with value 1 assigned to instants where the onset was exceeded and value 0 for the reminder. Applying the first order difference, the outcome 1 corresponded to instants of onset (increasing) values and -1 to instants of offset (decreasing). Initially, more than one value was assigned to both on and offset for each contraction because EMG signals oscillate. To obtain the unique and correct on and offset for each contraction, the algorithm had to remove all of the previously obtained by ensuring two things:

1. contraction minimally long - if between one onset and the correspondent offset, were present less than 1.6 seconds and the interval was to small to be considered a contraction, therefore these thresholds are ignored. The posterior onset and previous offset are kept.

2. relaxation minimally long - if between one offset and the posterior onset, was present less than 1 second, the interval of relaxation between these two assumed contractions was too short. Therefore, these are ignored and the contraction onset and the posterior offset are kept.

This procedure is performed for each signal. The resulting on and offset for each contraction are different among the signal collected from the right and from the left hand. To guarantee that these signals have commons intervals of contractions, it is chosen, for each contraction, the highest value from both onsets and the lowest from both offsets. Figure 4.1 shows in vertical black lines, the common on and offsets.

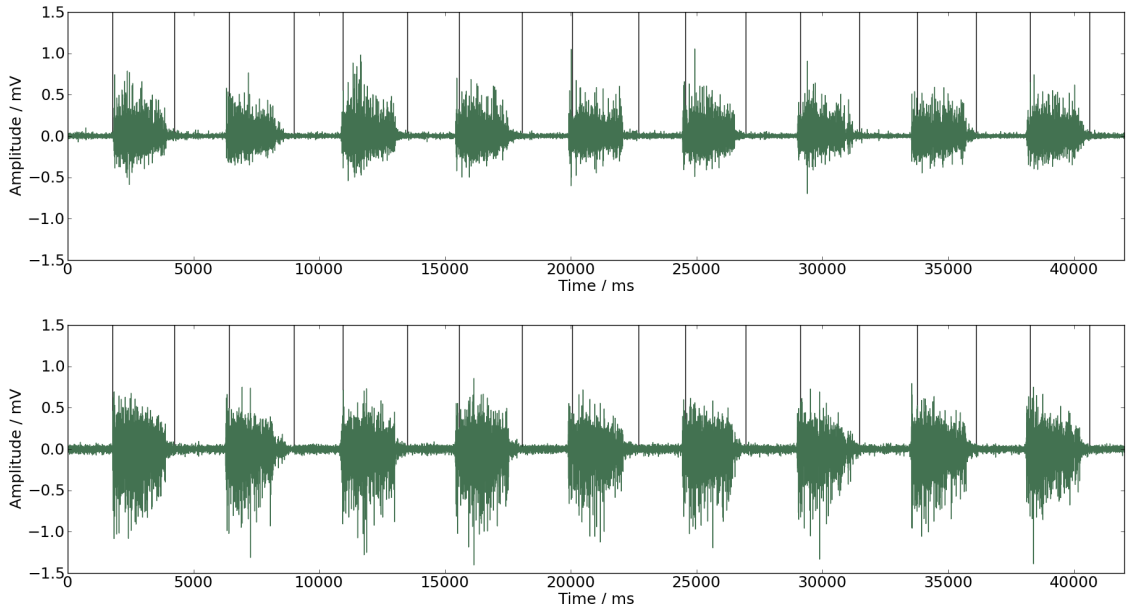

Figure 4.1: EMG signal with estimated common intervals of contraction. Black vertical lines represent on and offsets instants.

4.2 Hight-level Processing

4.2.1 Coherence Processing

As already mentioned in chapter 1.3, coherence between these EMG signals is better performed in periods of steady contraction. So, after low-level processing, using two long common sections of data from an interval of one contraction, coherence is calculated using equation 2.1. PSD for each section and Cross power spectral density (CSD) between both signals sections are estimated using Welch's average periodogram method from matplotlib.pyplot library. All EMG signals, with the purpose of coherence calculus, were full-wave rectified before any FFT was calculated. Sampling frequency is placed as 5 KHz, the Nonequispaced fast Fourier transform (NFFT) 1024, 2048 or 4096, and the value that dictates the dependency between FFT windows is half of NFFT value. The higher the NFFT chosen, the more precise will be the frequency resolution; making NFFT as 1024 yields a resolution of 4.88 Hz, as 2048 a resolution of 2.44 Hz and 4096 a resolution of 1.22 Hz. Preciser frequency resolution is preferable but having a lower precision allows to observe general trends.

Coherence is reported in two different ways. First, to provide a visual schematic representation of coherence dependency on frequency, coherence average among intervals

of contraction for a given muscle pair was performed across all patients within a group of subjects; this allows to precise coherence for each patient acquisition based on averaging multiple independent instants of data. Second, to provide an estimation of coherence dependency on frequency across the population of each group, mean coherence was calculated for the same values of frequency for a given muscle pair among all subjects within the same group. Alternatively, coherence was also calculated between both entire data in order to compare the influence of relaxation intervals. To assure that the wanted band of frequency was present in both signals of each patient, frequency spectra were computed, in two different ways. First, using numpy.fft library, discrete Fourier Transform was computed by Cooley-Tukey algorithm, to the entire collected data for each signal. Second, using matplotlib.pyplot library, PSD was computed with the same parameters used to perform coherence. Frequency spectra were calculated for all instants of contraction and then averaged to present an individual spectra for each patient. To refer that, even if the beta-band frequency is present does not mean that data is coherent within that same band, it means only that those frequencies exist in each signal.

4.2.2 PLF Processing

Since the beta-band frequencies are been studied, PLF was calculated for specific values of frequency f within this same band $[15, 30]$Hz with a resolution of 1 Hz. An example of filter used in this analysis is shown in figure 4.2(b). This procedure was performed among both control and patients group. Each signal was band pass filtered $[f-2, f+2]$, f being the analysed frequency, to eliminate from the signal all of the other undesirable frequencies. Instants of contraction where again isolated and for each, PLF calculated between each pair of ipsi and contralateral measurements.

Since is among instants of steady contraction that coherence is better estimated, PLF analysis was also performed for these same instants. Phase information is extracted from the EMG signals through the concept of *analytical signals*, which is performed by applying the Hilbert transform to the signal, for each pair of contractions. Hilbert transform was applied with resourcing to Fourier analysis using scipy.signal tools. Since the result of this transform is to convert each sample of acquisition into its corresponding imaginary numbers, phase between two contralateral signals can be calculated by finding each sample angle and subtracting them. This produces, for each instant of contraction, the

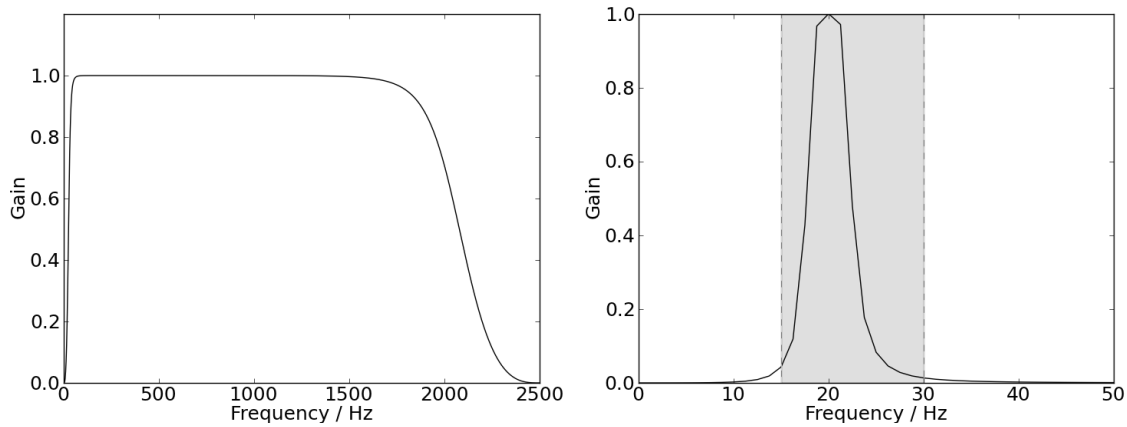

Figure 4.2: (a) Band pass filter $[15, 2000]$ Hz applied to all studied signals before processing. (b) Example of a band pass filter $[f-2, f+2]$ with f as 20 Hz, applied on a set of signals to calculate PLF for the given frequency of 20 Hz; delimited by the grey box, are represented the frequencies corresponding to beta-band.

difference of phase lag between them for each sample within all instant length. Therefore the portion $[\phi_j(t) - \phi_k(t)]$ from equation 2.2 is calculated and to present a ρ_{jk} value for each contraction, Euler formula is applied to each phase difference and averaged for all instants within the same contraction. This implies that, for each window of the pair signals, there is one PLF value. To present a final value for each member of each group, PLF was averaged between all contractions within the same acquisition. This procedure, as referred above, is performed as many times as the number of frequencies that are to be studied. PLF was averaged among all members within the same group to present a PLF value, dependent on frequency choice, for a population.

5

Results and Discussion

In this chapter are represented some validation tests using coherence analysis on basic signals and synthetic EMG signals. Coherence and PLF mean values results are presented for the algorithm used on acquired data from control and patients groups, for both ipsi and contralateral acquisitions. The aim is to verify whether significant changes occur between both groups of subjects.

5.1 Synthetic EMG Signals

For validation of the algorithms, synthetic EMG signals were used to compute coherence. To prove that coherence exists between two signals linearly dependent on each other for particular values of frequency, two different sets of signals were constructed and defined by equations 5.1 and 5.2:

$$signal = (sin(t \times 2\pi f) + k) \times n(t) \tag{5.1}$$

$$signal = (sin(t \times 2\pi f) + k) \times n(t) \times mod(t) \tag{5.2}$$

where, t is a sequence of integer numbers, incremented by one unit, with a desirable length; t is referred in seconds by dividing the desirable length for 5000, to take into

account the sampling frequency; $n(t)$ is a Gaussian noise ($\mu = 0$ and $\sigma = 1$), k the signal's envelope, f the signal's frequency and the portion $mod(t)$ present only in equation 5.2 (that determines the difference between both equations) represents the rest of the division of t by 6 bigger then 3 - guaranteeing instants of contraction and relaxation of 3000 ms.

An example with $t = 20s$ and $k = 3$ is shown in figure 5.1. In 5.1(a) is shown the signal created by equation 5.1 and in 5.1(b) is shown the signal created by equation 5.2.

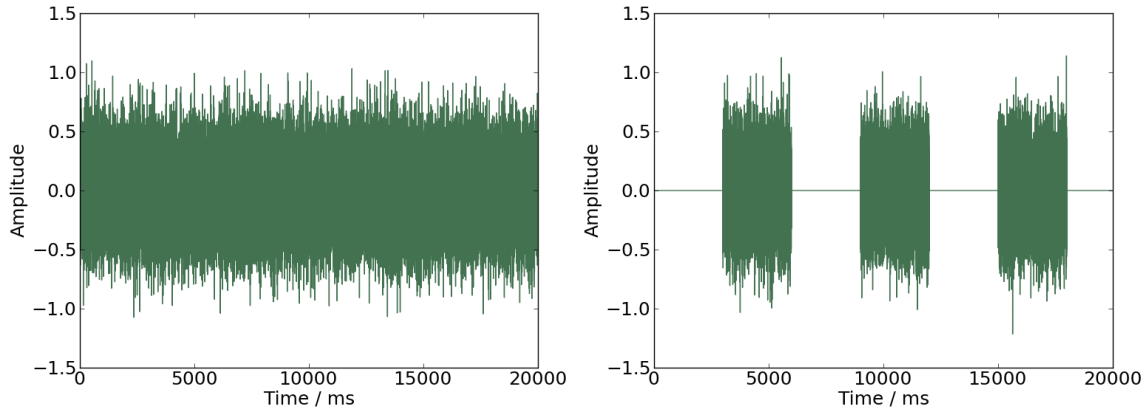

Figure 5.1: Schematic representation of the signal defined by equation 5.1 in (a), and the signal defined by equation 5.2 in (b).

Multiples signals were created, choosing t : 8, 80 or $391s$ and f : 10, 20 or 40 Hz. Number of samples were chosen to provide signals with 1, 13 and 65 contractions to decide the time sampling for acquisitions; frequency values were chosen taken into account that beta-band is being studied. For all signals created, coherence was calculated between two of the same type signals (simulating both right and left hands). Using signals defined by equation 5.2, coherence is performed for instants of contraction and then averaged for the entire measurement, unlike signals defined by equation 5.1, where coherence is calculated for the entire acquisition. The choice of NFFT won't be studied in this section since it only varies frequency resolution and on this particular signals its difference is not significant. Coherence results do not present any dependency on the choice of f value, since it assumes 1 for that frequency and near to 0 for the remaining. The results of frequency variation on both signals are presented in the example of figure 5.2.

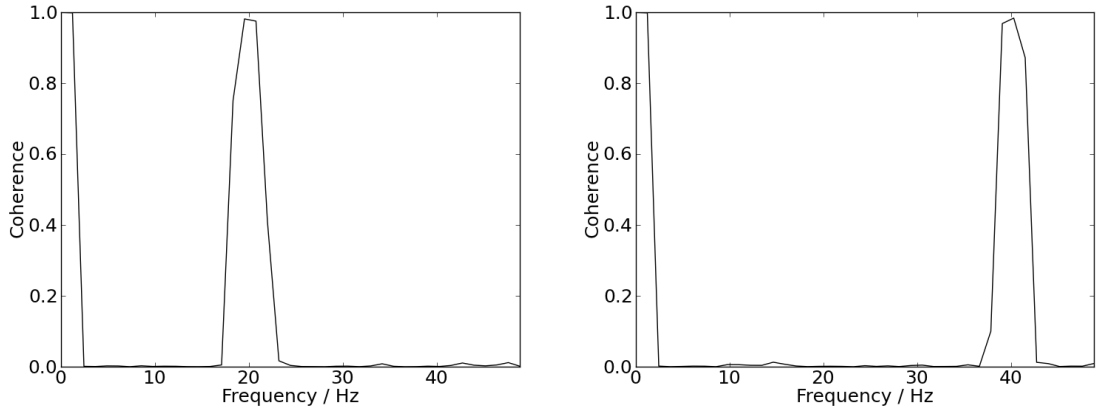

(a) (b)

Figure 5.2: (a) Coherence values for signals defined by equation 5.2 with f as 20Hz. (b) Coherence values for signals defined by equation 5.2 with f as 40Hz.

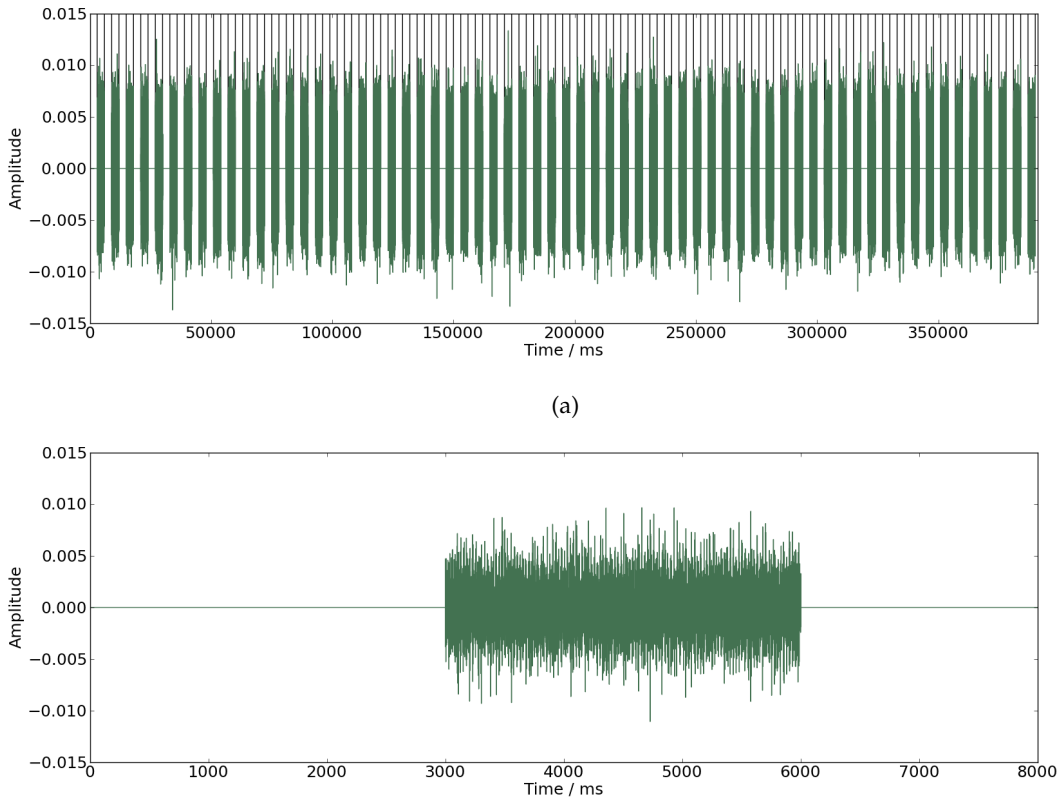

(a)

(b)

Figure 5.3: Signals defined by equation 5.2 with f placed as 40 Hz. (a) Signal with $391s$. (b) Signal with $8s$.

On the contrary, coherence results seem to depend on the choice of signals length. In figure 5.3 are represented two types of signals, both defined by equation 5.2, with

common value of 40 Hz for f but with different value of t. Figure 5.3(a) corresponds to a signal with 65 instants of contraction, while figure 5.3(b) represents a signal with 1 instant of contraction. For each type of signal referred in figure 5.3, two signals, with different portions of $n(t)$, were created to test coherence between them.

Results of mean coherence for these pair of signals can be observed in figure 5.4 and it is possible to affirm that the higher the signals length, the more accurate are the coherence results. It is possible to observe that in figure 5.4(b) coherence is different than 0; but the same phenomenon does not happen in figure 5.4(a). So, averaging coherence for greater amount of instants of contraction appears to reduce the coherence derived from the presence of noise (figure 5.4(b)), that only tends to disappear when not found among other contractions.

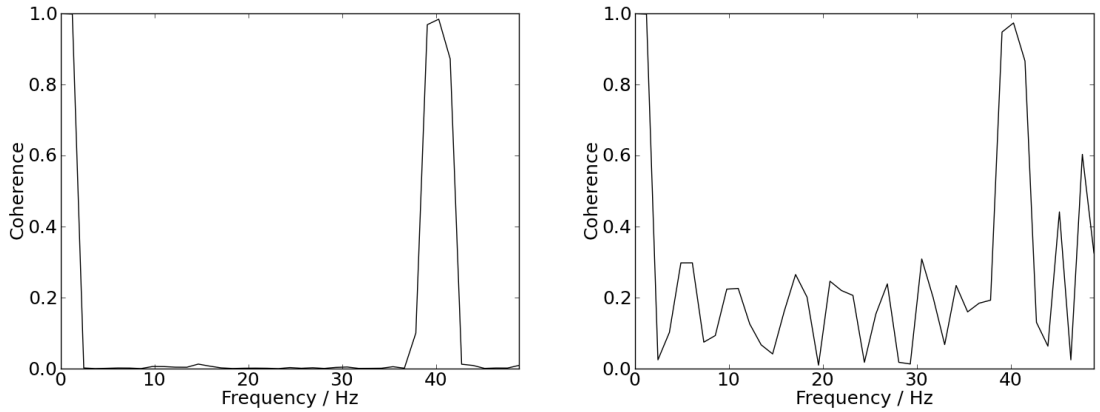

Figure 5.4: (a) Coherence values between two signals like those represented in figure 5.4(a). (b) Coherence values between two signals like those represented in figure 5.4(b).

These analyses were repeated for signals defined by equation 5.1. Varying frequency does not influences coherence general trends and results are similar with those presented in figure 5.2. But, as seen in 5.3, varying length alters coherence general trends.

For signals defined by equation 5.1, performed coherence for the entire signal is shown in figure 5.5.

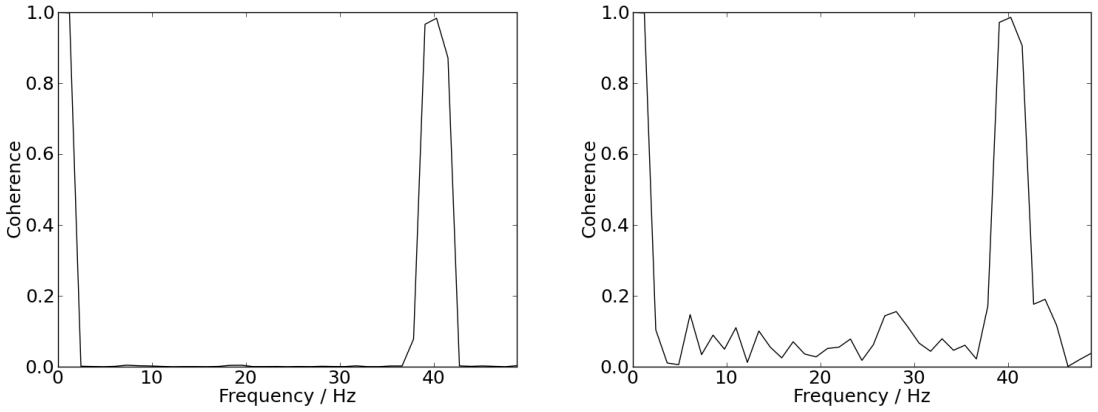

(a) (b)

Figure 5.5: Coherence values between two signals defined by equation 5.1 with f placed as 40 Hz. (a) Coherence for signals with $391s$. (b) Coherence for signals with $8s$.

Again, coherence comes more precise and accurate for signals with higher length. Differences between a signal defined by equation 5.2 - consistent of instants of contraction and relaxation - and a signal defined by equation 5.1 - consistent of only a contraction - arise for varying signals length, as shown in figures 5.4(a) and 5.5(a), respectively. Differences in coherence results between signals defined by equation 5.2 and 5.1 arise specially for long lengths, where coherence results are more accurate when averaged. It is possible to conclude, that is preferable to acquire data from higher sampling times and among reasonable number of contraction instants.

5.2 Coherence Tests

Some basic tests were performed to analyse the implemented code. Two random signals were used to test coherence between them and observe if resulted near 0 for all frequencies, once random signals do not present frequency synchronism between each other. Coherence was also tested between one signal and itself to observe if resulted exactly 1. These results are represented in figure 5.6. The choice of NFFT and the use of entire signal *vs.* instants of contractions, was not relevant because quantifying coherence was not the purpose, but to observe the general trends.

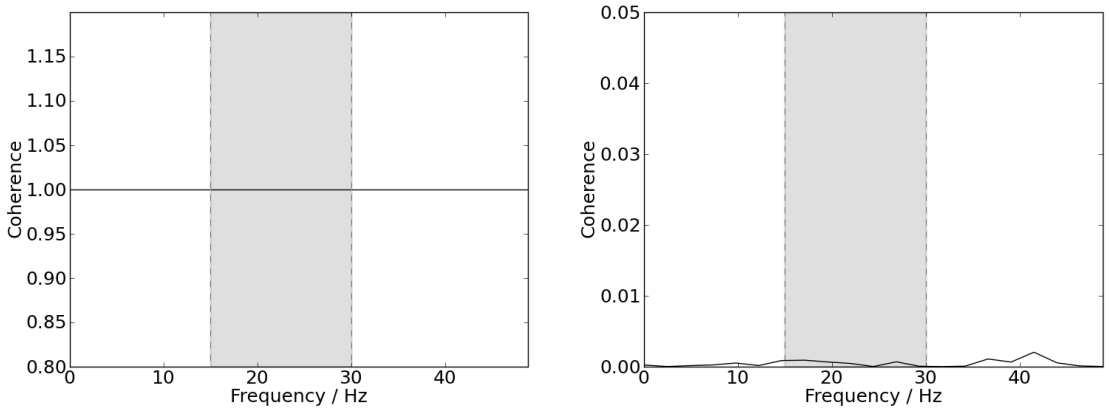

(a) (b)

Figure 5.6: (a) Coherence between one chosen signal and itself. (b) Coherence between two random signals. Both are calculated with NFFT as 4096.

5.3 Coherence Analysis

5.3.1 Ipsilateral

For both signals collected, ipsilateral coherence was analysed for instants of contraction using NFFT as 4096. Graphical representations are shown in figure 5.7.

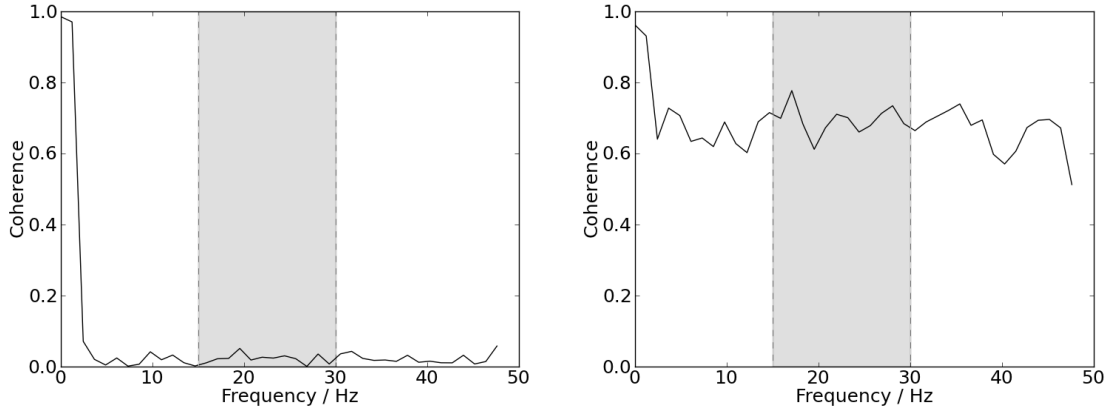

(a) (b)

Figure 5.7: (a) Ipsilateral coherence results acquired from the member of the group of patients. (b) Ipsilateral coherence results acquired from the member of the group of control. Delimited by the grey box are represented the frequencies corresponding to beta-band.

Analysing the results, it is possible to observe that the signal acquired from the patient presents coherence near 0 for all frequencies, while coherence from the control subject

presents high values for most presented frequencies, despite the fact that beta-band is not distinguished from the remaining frequencies. Differences are significant since for beta-band, coherence mean value for the patient was 0.0235 ± 0.0127 and for the control subject 0.6936 ± 0.0401.

Comparing the obtained results with those found in literature, it can be stated that coherence values associated to the patient acquisition were expected, since it was already reported a decrease on coherence for the beta-band among ALS patients [6]. However, results from the control group member are not expected since do not appear to be any close from those observed in literature, which are only slightly higher than those observed for patients, unlike the presented ones. Differences in results may be explained by differences in acquisition protocol, used algorithm or parameters.

5.3.2 Contralateral

Prior to coherence analysis, the presence of beta-band frequencies among all signals was tested, recurring to frequency spectrum analysis. Spectra were calculated in two different ways, and for both, results are represented as an average within all members from each group - control and patients. First, the entire signals were full wave rectified and its frequency spectrum calculated from FFT method, using Cooley–Tukey algorithm from scipy.fftpack library. In figures 5.8 and 5.9 are shown the graphical representations of each value of frequency intensity for patients and control group, respectively.

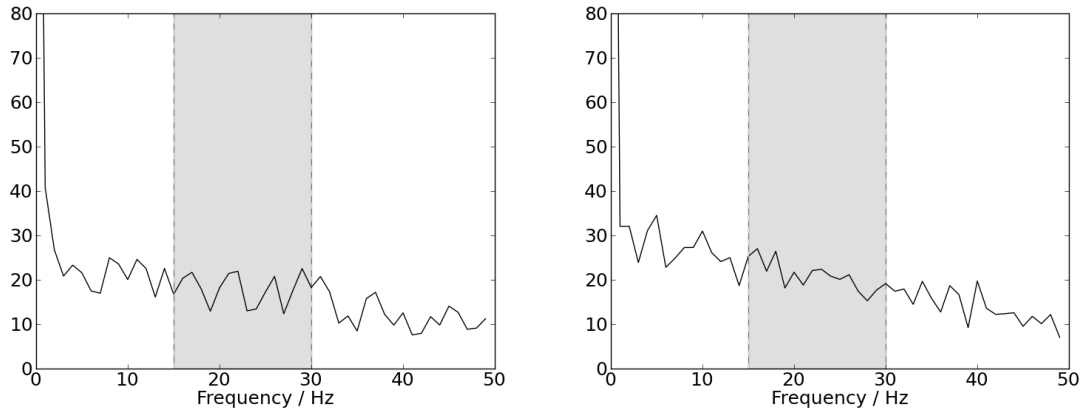

Figure 5.8: Schematic representation of frequency intensity dependency; delimited by the grey box are represented the frequencies corresponding to beta-band. (a) Results for the group of patients collected from the left hand. (b) Results for the group of patients collected from the right hand.

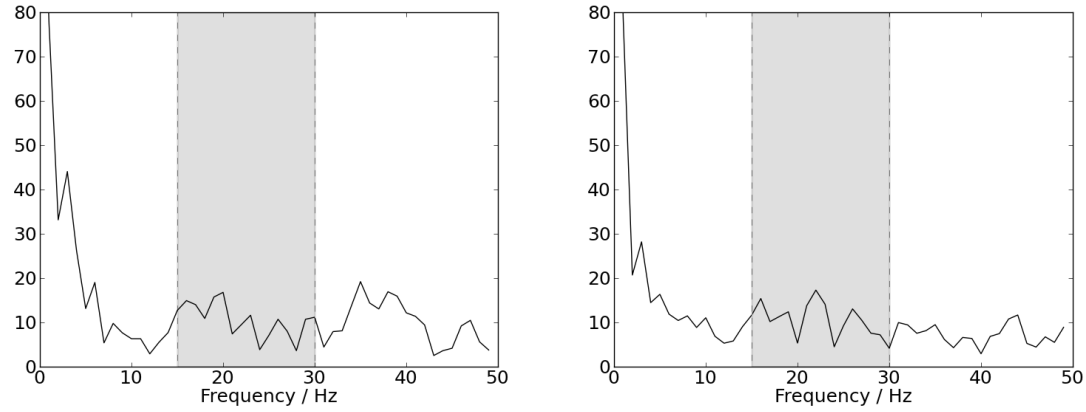

Figure 5.9: Schematic representation of frequency intensity dependency; delimited by the grey box, are represented the frequencies corresponding to beta-band. (a) Results for the control group collected from the left hand. (b) Results for the control group collected from the right hand.

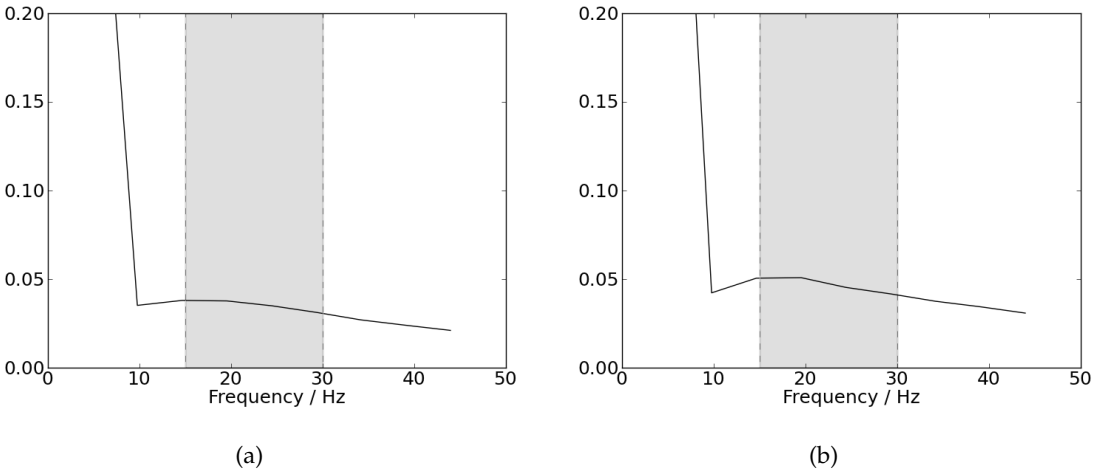

Figure 5.10: Schematic representation of frequency intensity dependency assuming NFFT as 1024; delimited by the grey box are represented the frequencies corresponding to beta-band. (a) Results for the group of patients collected from the left hand. (b) Results for the group of patients collected from the right hand.

As observable in figures 5.8 and 5.9, the beta-band frequencies do not stand out from the remaining existent frequencies in neither hand or group; it is possible to conclude that searching for beta-band among entire signals is not viable. Thus, as performed for coherence, the instants of muscular contraction were isolated, its frequency spectra calculated for full-wave rectified instants, for a variable NFFT value, and averaged within all contractions to present a single result for each measurement; these frequency spectra were

performed by PSD calculus resorting to Welch's average periodogram method from matplotlib.pyplot library. Graphical representations of these results for patients group are shown in figures 5.10 and 5.12, and for control group in figures 5.11 and 5.13, for NFFT as 1024 and 2048 respectively. A different value of NFFT only changes the prospectives to sight and general trends.

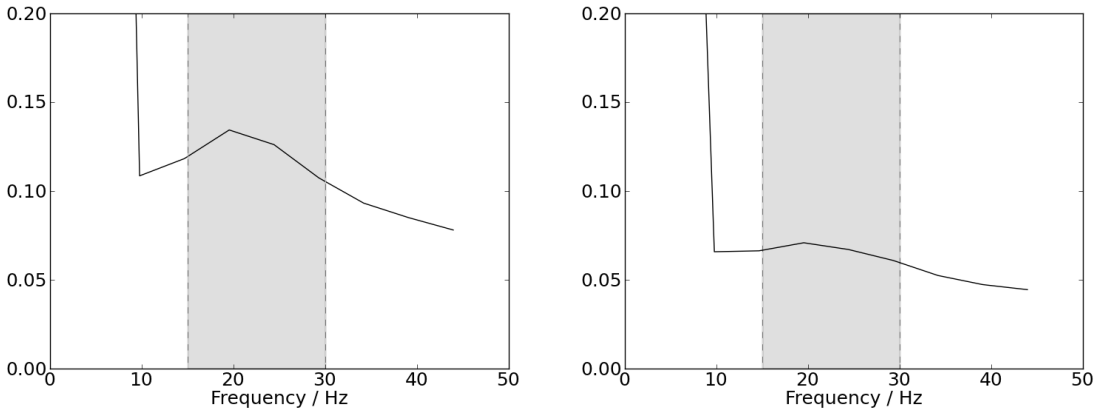

(a) (b)

Figure 5.11: Schematic representation of frequency intensity dependency assuming NFFT as 1024; delimited by the grey box are represented the frequencies corresponding to beta-band. (a) Results for the control group collected from the left hand. (b) Results for the control group collected from the right hand.

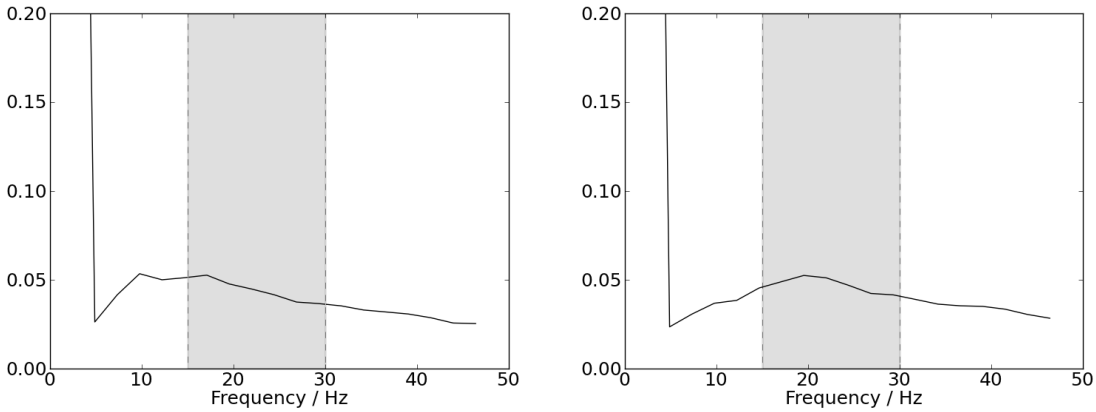

(a) (b)

Figure 5.12: Schematic representation of frequency intensity dependency assuming NFFT as 2048; delimited by the grey box are represented the frequencies corresponding to beta-band. (a) Results for the group of patients collected from the left hand. (b) Results for the group of patients collected from the right hand.

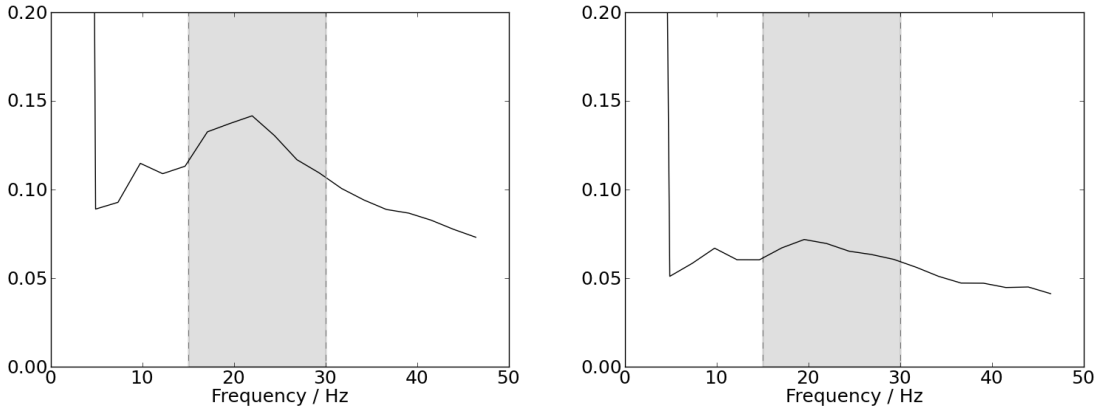

Figure 5.13: Schematic representation of frequency intensity dependency assuming NFFT as 2048; delimited by the grey box are represented the frequencies corresponding to beta-band. (a) Results for the control group collected from the left hand. (b) Results for the control group collected from the right hand.

In figures 5.10 - 5.13, results show a higher presence of beta-band frequencies, since they appear more enhanced than the remaining, for the majority of all results from both hands and groups. When a frequency spectrum is calculated on instants of contraction and within the same group averaged, it can be concluded that beta-band is present among signals and it would be reasonable to expect coherence existence. The same can not be proved for an entire signal, with instants of relaxation included, since frequency spectrums in figures 5.9 and 5.8 show that the analysis of the entire signals do not enhance the beta-band frequencies. Therefore, as already proved in the literature, and showed for these signals, instants of steady contraction are better indicators for beta-band analysis.

As shown in chapter 5.3.1, ipsilateral coherence is a precise indicator of neuronal degeneration development. Contralateral coherence is tested to check whether results are similar to those obtained for ipsilateral acquisitions. Contralateral coherence between both interosseous muscles, one from each side, are shown for patients and control subjects groups in figures 5.14(a) and 5.14(b), respectively. The results of coherence dependency on frequency for both groups using NFFT as 1024 are summarized in figure 5.14 and tables 5.1 and 5.2.

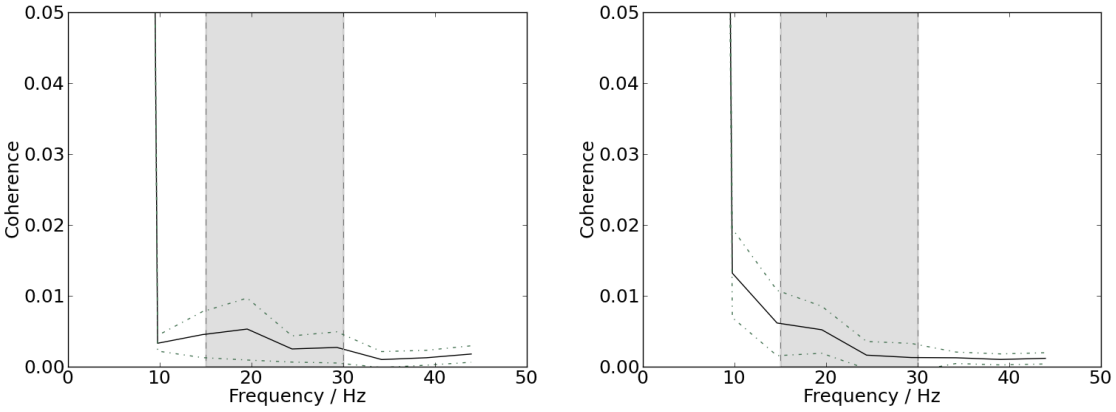

(a) (b)

Figure 5.14: Schematic representation of mean coherence dependency on frequency by the straight line and standard deviation by the dotted line, with NFFT placed at 1024; delimited by the grey box are represented the frequencies corresponding to beta-band. (a) Results from the group of patients. (b) Results from the control group.

Frequency / Hz	**14.65**	**19.53**	**24.41**	**29.30**
Mean Coherence ($x10^{-03}$)	4.53	5.31	2.50	2.72
Standard deviation ($x10^{-03}$)	3.24	4.37	1.85	2.20

Table 5.1: For each frequency, among the beta-band, are represented mean coherence values and standard deviation for the group of patients, with NFFT placed as 1024.

Frequency / Hz	**14.65**	**19.53**	**24.41**	**29.30**
Mean Coherence ($x10^{-03}$)	6.16	5.21	1.63	1.29
Standard deviation ($x10^{-03}$)	4.61	3.31	1.93	1.99

Table 5.2: For each frequency, among the beta-band, are represented mean coherence values and standard deviation for the group of subjects, with NFFT placed as 1024.

The same analysis and results are represented for the group of patients and the control group using NFFT as 2048, in figure 5.15 and in tables 5.3 and 5.4, respectively.

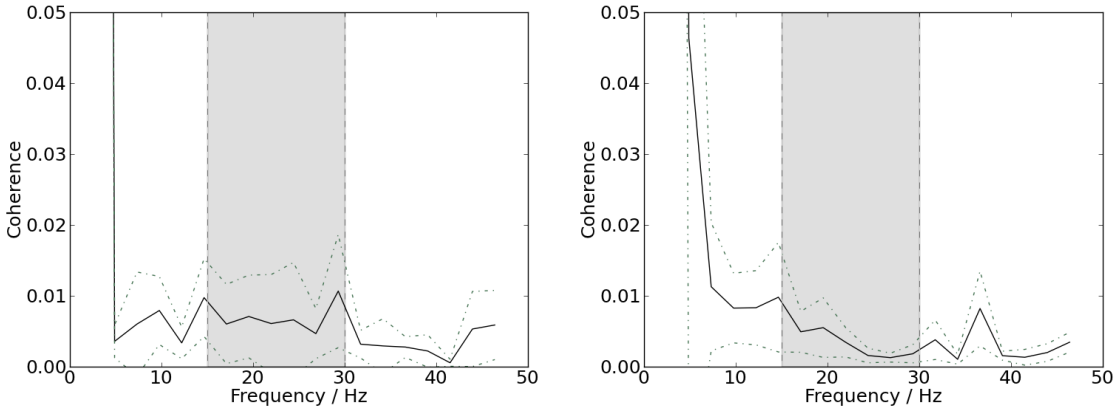

Figure 5.15: Schematic representation of mean coherence dependency on frequency by the straight line and standard deviation by the dotted line, with NFFT placed at 2048; delimited by the grey box, are represented the frequencies corresponding to beta-band. (a) Results from the group of patients. (b) Results from the group of subjects.

Frequency / Hz	**14.65**	**17.09**	**19.53**	**21.97**	**24.41**	**26.86**	**29.30**
Mean Coherence ($x10^{-03}$)	9.75	6.02	7.08	6.09	6.61	4.67	10.67
Standard deviation ($x10^{-03}$)	5.49	5.59	5.84	6.91	8.09	3.54	7.98

Table 5.3: For each frequency, among the beta-band, are represented mean coherence values and standard deviation for the group of patients.

Frequency / Hz	**14.65**	**17.09**	**19.53**	**21.97**	**24.41**	**26.86**	**29.30**
Mean Coherence ($x10^{-03}$)	9.81	4.92	5.51	3.45	1.58	1.28	1.82
Standard deviation ($x10^{-03}$)	7.73	2.89	4.20	2.07	1.03	0.63	1.28

Table 5.4: For each frequency, among the beta-band, are represented mean coherence values and standard deviation for the group of patients.

Using NFFT as 4096, it is only possible to present results for the group of subjects, that can be seen in figure 5.16 and in table 5.5. Since the group of patients present more difficulties in maintaining a definite contraction with a certain force, intervals of contraction are smaller when compared to those observed in control subjects signals and it becomes impossible to analyse them without creating zero-patting effect.

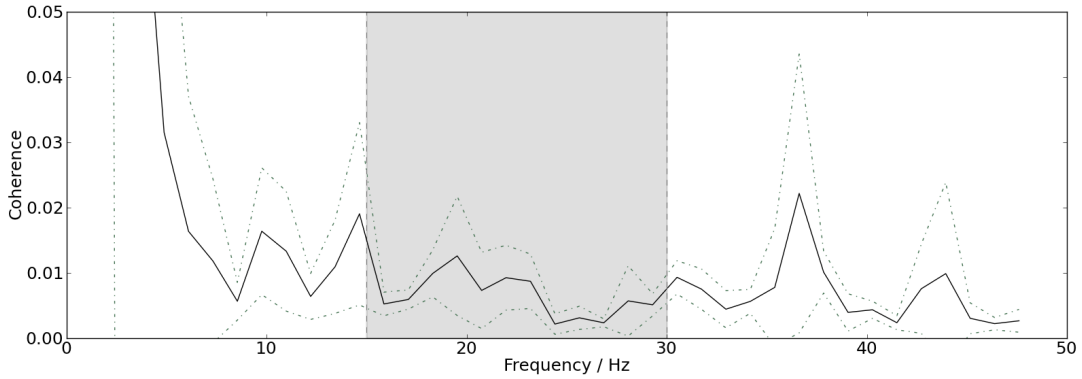

Figure 5.16: Schematic representation of mean coherence dependency on frequency by the straight line and standard deviation by the dotted line, with NFFT placed at 4096 for the group of subjects; delimited by the grey box, is represented the frequencies corresponding to beta-band.

Frequency / Hz	**14.65**	**15.87**	**17.09**	**18.31**	**19.53**	**20.75**	**21.97**
Mean Coherence ($x10^{-03}$)	19.06	5.24	5.93	9.92	12.61	7.32	9.27
Standard deviation ($x10^{-03}$)	13.97	1.81	1.47	3.60	9.13	5.85	4.97
Frequency / Hz	**23.19**	**24.41**	**25.63**	**26.86**	**28.08**	**29.30**	**30.52**
Mean Coherence ($x10^{-03}$)	8.72	2.16	3.12	2.36	5.71	5.12	9.33
Standard deviation ($x10^{-03}$)	4.16	1.57	1.78	0.61	5.38	1.70	2.55

Table 5.5: For each frequency, among the beta-band, are represented mean coherence values and standard deviation for the group of patients.

Results from the control group are not entirely similar to those observed in literature. Coherence for the beta-band frequencies does not stand out from the presented in the remaining frequencies. There was no significant coherence present for any of the acquisitions from the group of subjects, since for beta-band, pooled coherence value for the patients group was 0.0069 ± 0.0019 and for the control group 0.0031 ± 0.0017 (using NFFT as 2048). Coherence was present within significance (in the same order of magnitude found in literature), but not higher on the beta-band than the remaining frequencies.

The analysis from the group of patients show a behaviour similar to the group of patients. Once again, intermuscular coherence was not considered significant within the beta-band. For both groups of subjects, coherence appears higher for lower frequencies (<10 Hz). This predominance will not be discussed, since its origin seems to be related

to trends on slow components of the signals, instead of beta-band interesting frequencies. Therefore, despite the possible presence of these frequencies (beta-band) on both signals, they do not significantly depend linearly from each other. Contralateral coherence between coactivated muscles from left and right side are not significant within the beta-band. Regardless of the chosen value for NFFT, contralateral coherence should not be used to search the beta-band and can not be used to reflect the degeneration of corticospinal pathways.

5.4 PLF Analysis

5.4.1 Ipsilateral

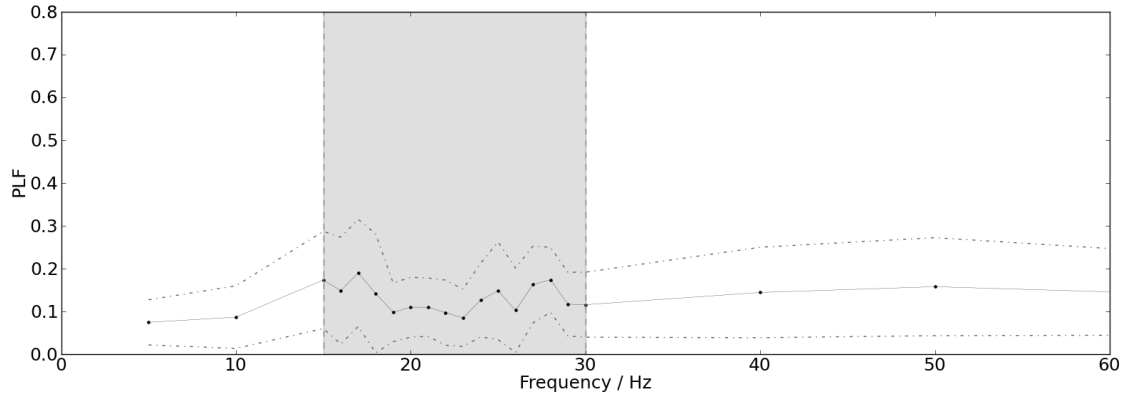

(a)

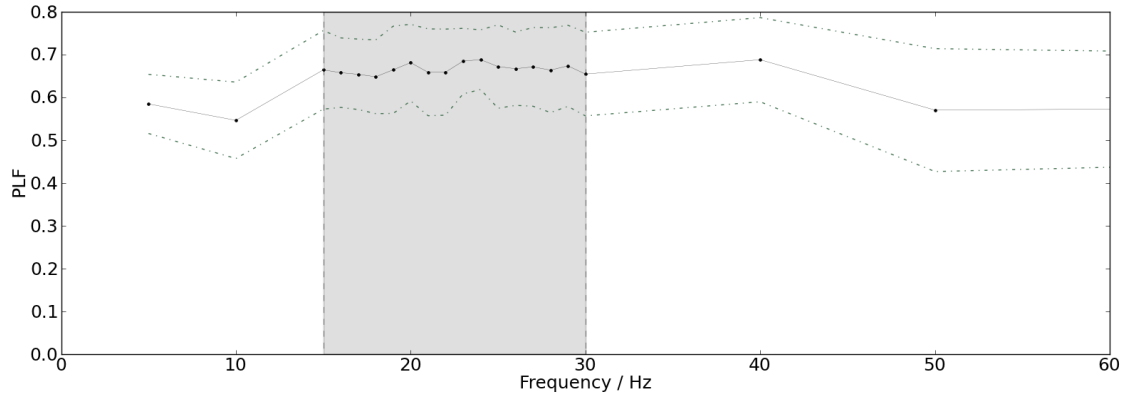

(b)

Figure 5.17: Schematic representation of mean PLF values dependency on frequency by the straight line and standard deviation by the dotted line, for ipsilateral acquisitions; delimited by the grey box are represented the frequencies corresponding to beta-band. (a) Results from the group of patients. (b) Results from the control group.

As performed for ipsilateral coherence analysis, PLF was estimated for both subjects. The development and processing these signals was the same used in chapter 4; the frequencies of interest and its respective PLF values are represented in figure 5.17.

In figure 5.17(a) is visible that results are similar to those obtained in section 5.3.2. PLF values do not stand out from the remaining in beta-band and do not assume significant values for any frequency. On the other hand, observing figure 5.17(b), PLF assumes much higher values and beta-band frequencies appears to stand out from the remaining. Differences are significant since for beta-band, PLF mean value for the patient was 0.1312 ± 0.0310 and for the control subject 0.6664 ± 0.0093.

5.4.2 Contralateral

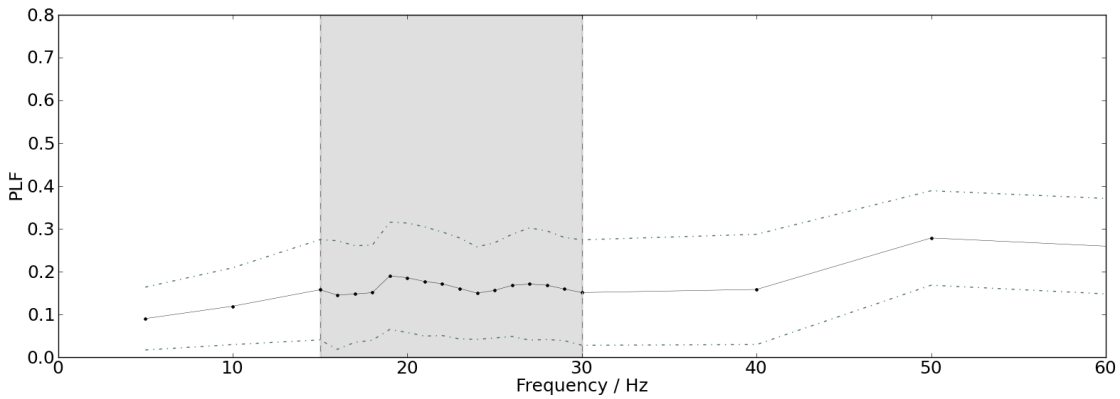

(a)

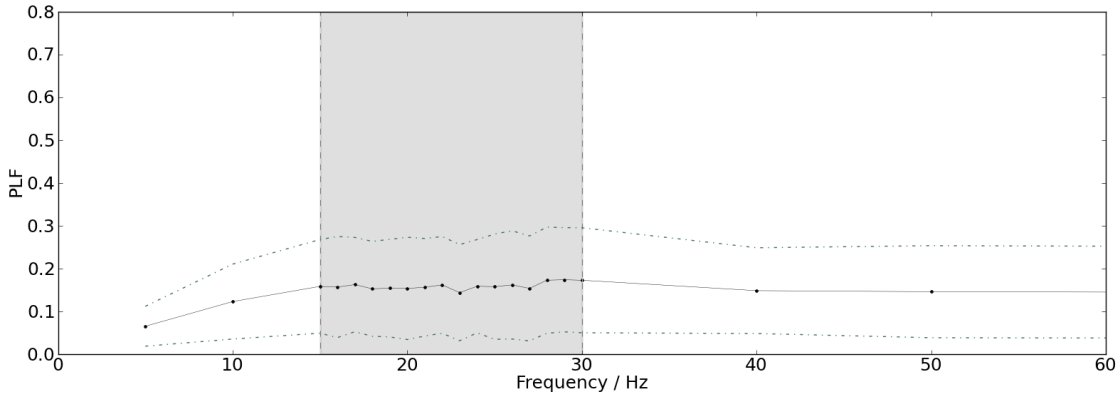

(b)

Figure 5.18: Schematic representation of mean PLF values dependency on frequency by the straight line and standard deviation by the dotted line, for contralateral acquisitions; delimited by the grey box are represented the frequencies corresponding to beta-band. (a) Results from the group of patients. (b) Results from the control group.

Contralateral analysis is represented in figure 5.18, where mean values of PLF depending on frequency are visible, for the group of patients and of control in 5.18(a) and 5.18(b), respectively.

As observed in both graphics representations of figure 5.18, PLF values do not significantly stand out for the beta-band frequencies, since for beta-band, PLF pooled value for the patients group was 0.1205 ± 0.0068 and for the control subject 0.1169 ± 0.0057.

5.5 One Long Contraction

To test if determining coherence by mean values from various contractions is more accurate than studying just one (not using averages values) frequency and time domain tests were performed on one long contraction ($\approx$ 10 s) from contra and ipsilateral acquisitions. This test was performed 4 times, only applied to one member from the control group. An example of signal acquired is represented in figure 5.19.

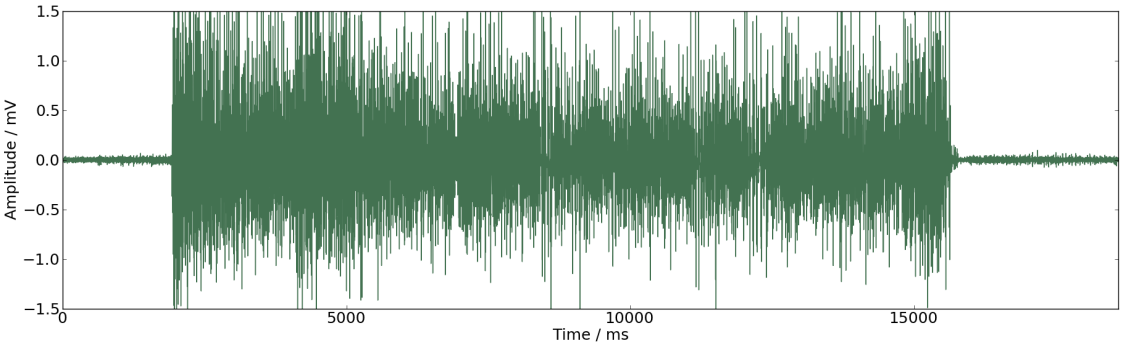

Figure 5.19: Signal acquired from a member of the control group, consisting in one long muscle contraction.

For both contra and ipsilateral measurements, coherence was analysed between two signals of the same type for the entire instant of contraction. NFFT was placed as 4096 for all analysis. In figure 5.20 are represented mean coherence values from the acquisitions performed on the member from the control group.

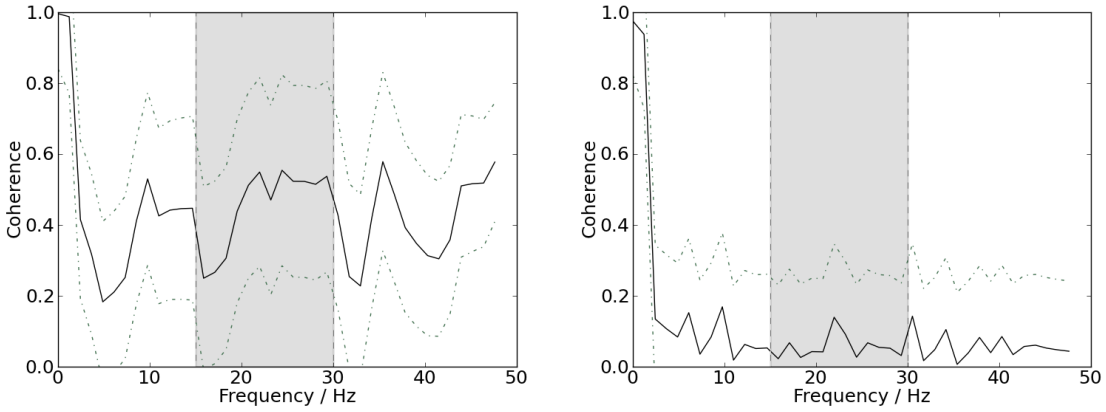

(a) (b)

Figure 5.20: Schematic representation of mean coherence values dependency on frequency by the straight line and standard deviation by the dotted line; delimited by the grey box are represented the frequencies corresponding to beta-band. (a) Results from ipsilateral acquisitions. (b) Results from contralateral acquisitions.

As expected, these obtained results do not appear to be significantly different from those obtained in chapter 5.3: contralateral coherence shows again low and insignificant levels of coherence for all frequencies, while ipsilateral coherence shows higher levels of coherence. Differences are significant since for beta-band, coherence mean value in contralateral acquisitions is 0.0576 ± 0.0327 and in ipsilateral acquisitions is 0.4462 ± 0.1105.

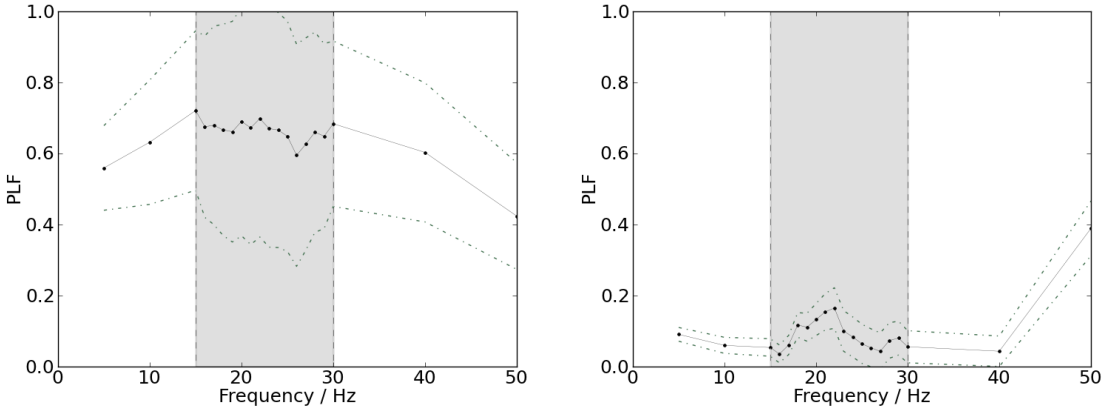

(a) (b)

Figure 5.21: Schematic representation of PLF mean values dependency on frequency by the straight line and standard deviation by the dotted line; delimited by the grey box are represented the frequencies corresponding to beta-band. (a) Results from ipsilateral acquisitions. (b) Results from contralateral acquisitions.

PLF was analysed between two signals from the same type for the instant of contraction. In 5.21 are represented mean PLF values for the long instant of contraction, for both contra and ipsilateral acquisitions.

PLF results do not appear to be significantly different from those obtained in chapter 5.4: contralateral PLF shows low and insignificant levels for all frequencies, while ipsilateral PLF shows higher levels. Differences are significant since for beta-band, PLF mean value in contralateral acquisitions is 0.0885 ± 0.0388 and in ipsilateral acquisitions is 0.6652 ± 0.0286.

To conclude this analysis, as previously seen in chapter 5.3 and 5.4, ipsilateral results are higher than contralateral ones, for both coherence and PLF analysis. As already expected by analysis in chapter 5.1, averaging coherence values among instants of contraction presents more accurate results and therefore, is preferable to use long sampling times. Comparing, for example, ipsilateral coherence among the group of control for the beta-band, using long sampling times results in coherence mean values of 0.6936 ± 0.0401, while using only one long instant of contraction results in coherence mean values of 0.4462 ± 0.1105.

6

Conclusions

In muscular activity, beta-band frequencies allegedly occur as a result of common cortical drive. The presence of this band dictates the condition of neuronal pathways and could be used for sensorimotor processing [6], since it has been demonstrated that these oscillations and coupling between them disappear after stroke and complete spinal cord injury [6].

In this work, a methodology has been developed to evaluate the level of coherence and synchronism of different muscles groups in patients presenting ALS and in control subjects. To begin with, some tests were performed to validate signals processing. Tests of coherence were applied to random signals and coherence assumes values near 0; coherence tests were performed between a signal and itself and coherence assumes 1. Both tests confirm that coherence behaves as supposed to through the developed processing, guaranteeing that was correctly applied. Synthetic EMG signals with a specific known value of frequency were used to test coherence between two signals of the same type, to find whether coherence among them is present for that same frequency. Two types of analyses were used, one consisting in a pair of signals with instants of contraction and relaxation and other pair consisting in signals of an entire contraction. For both sets of signals, setting a frequency, mean coherence values between two signals for the same type are close to 1 for the specific frequency and near 0 for the remaining. So, varying signals frequency value does not change coherence general trends. But, altering these

signals length, changes the number of instants of contraction used to present final averaged coherence, and the lower the number of samples, the higher will be the influence of noise. Differences in coherence results between both sets of signals arise specially for longer lengths, where coherence results are more accurate when averaged. It is possible to conclude, that is preferable higher sampling times among a reasonable number of contraction instants.

Both coherence and PLF analysis in ipsilateral acquisitions present significant differences between both groups of patients, as already proved in previous publications. Results from the group of patients present no significant differences from the results obtained for contralateral acquisitions but the group of subjects presents higher values of PLF and coherence for all frequencies, specially for beta-band. So, it is possible to assume that while control subjects present no neuronal or muscular anomalies and therefore higher synchrony for beta -band, patients with ALS do not present synchrony in any frequency, specially for beta-band.

The results allow to conclude that ipsilateral analysis is a good measure of corticospinal pathways integrity. Frequency spectra were performed for contralateral acquisitions and it was demonstrated that beta-band frequencies are present in instants of steady contraction. But, as proved by coherence and PLF analysis beta-band frequencies in contralateral acquisitions was not present in neither, for patients or control subjects. Neither differences or significance values were found for both control and patients groups. Therefore, it is to conclude that contralateral frequency analysis is not a good marker for beta-band frequencies studies.

Concerning the distributions of PLF values measured from patients and control subjects, presenting a clear difference between both for ipsilateral acquisitions, it is affirmed that ipsilateral measurements reflect neuronal degeneration. So, PLF analysis may have potential as a quantitative test of upper and lower neuron integrity related to ALS.

Some limitations may be associated with this present work. The amount of acquired and analysable EMG signals was not enough to arrange groups with significant number of subjects. For PLF analysis, the used band pass filters could not be applied to ignore all frequencies but the wanted one and the filter region comprehended an interval of $[f-2, f+2]$ (not as straight as wanted), f being the analysed frequency. Comparing both methods used to study frequency and time domains, PLF analysis may be seen as a more practical method since it requires smaller sections of data, compared to coherence. On the

other hand, PLF can only be analysed for a specific value of frequency, while coherence is analysed for the range of frequencies presented on data. To conclude, as further work is suggested to rely on the possibility of using PLF analysis to observe beta-band and assess about neuronal pathways integrity in ipsilateral acquisitions. Therefore, it seems possible that PLF may be used as a method of diagnosing ALS.

Bibliography

[1] Raafat El-Sayed Shalaby. *Development of an Electromyography Detection System for the Control of Functional Electrical Stimulation in Neurological Rehabilitation*. PhD thesis, Universitätsbibliothek, 2011.

[2] Matthew C Kiernan, Steve Vucic, Benjamin C Cheah, Martin R Turner, Andrew Eisen, Orla Hardiman, James R Burrell, and Margaret C Zoing. Amyotrophic lateral sclerosis. *The Lancet*, 377(9769):942–955, 2011.

[3] Bryan J Traynor, Mary B Codd, Bernadette Corr, Colm Forde, Eithne Frost, and Orla M Hardiman. Clinical features of amyotrophic lateral sclerosis according to the el escorial and airlie house diagnostic criteria: a population-based study. *Archives of neurology*, 57(8):1171, 2000.

[4] Asa J Wilbourn. Clinical neurophysiology in the diagnosis of amyotrophic lateral sclerosis: the lambert and the el escorial criteria. *Journal of the neurological sciences*, 160:S25–S29, 1998.

[5] Mamede de Carvalho, Reinhard Dengler, Andrew Eisen, John D England, Ryuji Kaji, Jun Kimura, Kerry Mills, Hiroshi Mitsumoto, Hiroyuki Nodera, Jeremy Shefner, et al. Electrodiagnostic criteria for diagnosis of als. *Clinical Neurophysiology*, 119(3):497–503, 2008.

[6] Karen M Fisher, Boubker Zaaimi, Timothy L Williams, Stuart N Baker, and Mark R Baker. Beta-band intermuscular coherence: a novel biomarker of upper motor neuron dysfunction in motor neuron disease. *Brain*, 135(9):2849–2864, 2012.

[7] JD Mitchell and GD Borasio. Amyotrophic lateral sclerosis. *The lancet*, 369(9578):2031–2041, 2007.

[8] Mamede de Carvalho, Antónia Turkman, and Michael Swash. Motor unit firing in amyotrophic lateral sclerosis and other upper and lower motor neurone disorders. *Clinical Neurophysiology*, 2012.

[9] Simon F Farmer, John Gibbs, David M Halliday, Linda M Harrison, Leon M James, Margaret J Mayston, and John A Stephens. Changes in emg coherence between long and short thumb abductor muscles during human development. *The Journal of physiology*, 579(2):389–402, 2007.

[10] Stuart Nicolas Baker, R Spinks, A Jackson, and RN Lemon. Synchronization in monkey motor cortex during a precision grip task. i. task-dependent modulation in single-unit synchrony. *Journal of Neurophysiology*, 85(2):869–885, 2001.

[11] Stuart N Baker, Matthew Chiu, and Eberhard E Fetz. Afferent encoding of central oscillations in the monkey arm. *Journal of neurophysiology*, 95(6):3904–3910, 2006.

[12] Wolfgang Klimesch, Roman Freunberger, Paul Sauseng, and Walter Gruber. A short review of slow phase synchronization and memory: evidence for control processes in different memory systems? *Brain research*, 1235:31–44, 2008.

[13] Carla Cordivari, Andrew J Lees, V Peter Misra, and Peter Brown. Emg–emg coherence in writer's cramp. *Movement disorders*, 17(5):1011–1016, 2002.

[14] BA Conway, DM Halliday, SF Farmer, U Shahani, P Maas, AI Weir, and JR Rosenberg. Synchronization between motor cortex and spinal motoneuronal pool during the performance of a maintained motor task in man. *The Journal of Physiology*, 489(Pt 3):917–924, 1995.

[15] Tatsuya Mima and Mark Hallett. Electroencephalographic analysis of cortico-muscular coherence: reference effect, volume conduction and generator mechanism. *Clinical neurophysiology*, 110(11):1892–1899, 1999.

[16] Naja L Hansen, Bernard A Conway, David M Halliday, Simon Hansen, Henrik S Pyndt, F Biering-Sørensen, and Jens B Nielsen. Reduction of common synaptic drive to ankle dorsiflexor motoneurons during walking in patients with spinal cord lesion. *Journal of neurophysiology*, 94(2):934–942, 2005.

[17] Mamede de Carvalho. Testing upper motor neuron function in amyotrophic lateral sclerosis: the most difficult task of neurophysiology. *Brain*, 135(9):2581–2582, 2012.

[18] Andrew Jackson, RL Spinks, TCB Freeman, DM Wolpert, and RN Lemon. Rhythm generation in monkey motor cortex explored using pyramidal tract stimulation. *The Journal of Physiology*, 541(3):685–699, 2004.

[19] C Nicholas Riddle and Stuart N Baker. Manipulation of peripheral neural feedback loops alters human corticomuscular coherence. *The Journal of physiology*, 566(2):625–639, 2005.

[20] Jacques Duchateau and Roger M Enoka. Human motor unit recordings: origins and insight into the integrated motor system. *Brain research*, 1409:42–61, 2011.

[21] Paulo Henrique Marchetti and Marcos Duarte. Instrumentação em eletromiografia. *Laboratório de Biofísica, Escola de Educação Física e Esporte. São Paulo: Universidade de São Paulo*, 2006.

[22] François Hug and Sylvain Dorel. Electromyographic analysis of pedaling: a review. *Journal of electromyography and kinesiology: official journal of the International Society of Electrophysiological Kinesiology*, 19(2):182, 2009.

[23] David M Halliday, Bernard A Conway, Simon F Farmer, and Jay R Rosenberg. Using electroencephalography to study functional coupling between cortical activity and electromyograms during voluntary contractions in humans. *Neuroscience letters*, 241(1):5–8, 1998.

[24] JF Marsden, P Ashby, P Limousin-Dowsey, JC Rothwell, and P Brown. Coherence between cerebellar thalamus, cortex and muscle in man cerebellar thalamus interactions. *Brain*, 123(7):1459–1470, 2000.

[25] Yukio Nishimura, Yosuke Morichika, and Tadashi Isa. A subcortical oscillatory network contributes to recovery of hand dexterity after spinal cord injury. *Brain*, 132(3):709–721, 2009.

[26] D Stegeman and H Hermens. Standards for surface electromyography: The european project surface emg for non-invasive assessment of muscles (seniam). *Línea). Disponible en: http://www. med. uni-jena. de/motorik/pdf/stegeman. pdf [Consultado en agosto de 2008]*, 2007.

[27] P Grosse, MJ Cassidy, P Brown, et al. Eeg-emg, meg-emg and emg-emg frequency analysis: physiological principles and clinical applications. *Clinical neurophysiology: official journal of the International Federation of Clinical Neurophysiology*, 113(10):1523, 2002.

[28] Pascal Grosse, M Edwards, MAJ Tijssen, A Schrag, Andrew J Lees, KP Bhatia, and Peter Brown. Patterns of emg–emg coherence in limb dystonia. *Movement disorders*, 19(7):758–769, 2004.

[29] Jose M Hurtado, Leonid L Rubchinsky, and Karen A Sigvardt. Statistical method for detection of phase-locking episodes in neural oscillations. *Journal of neurophysiology*, 91(4):1883–1898, 2004.

[30] Miguel Almeida, Ricardo Vigário, and J Bioucas-Dias. Phase locked matrix factorization. In *Proc. of the EUSIPCO Conference*, 2011.

7

Appendix

On this appendix are presented the papers written throughout this thesis. The first developed paper is entitled 'A method to detect keystrokes using accelerometry to quantify typing rate and monitor neurodegenerative progression' submitted and accepted in conference NEUROTECHNIX 2013 as a Short Paper with a 20 minutes oral presentation. The second paper is entitled 'Coherence and Phase Locking Disruption in Electromyograms of Patients with Amyotrophic Lateral Sclerosis' and represents the work and results obtained in this thesis. This paper was submitted to BIOSIGNALS 2014 conference.

A method to detect keystrokes using accelerometry to quantify typing rate and monitor neurodegenerative progression

Ana Londral[1], Mafalda Câmara[2], Hugo Gamboa[2], Mamede de Carvalho[1,3], Anabela Pinto[1,3], Luís Azevedo[4]

[1]*Instituto de Medicina Molecular, Faculdade de Medicina, Universidade de Lisboa, Lisbon, Portugal*
[2]*Faculdade de Ciências e Tecnologia, Universidade Nova de Lisboa, Lisbon, Portugal*
[3]*Hospital de Santa Maria, Lisbon, Portugal*
[4]*Instituto Superior Técnico, Lisbon, Portugal*

Keywords: Progressive neurological conditions, motor performance, assistive technologies, accelerometer, Amyotrophic Lateral Sclerosis

Abstract: Progressive motor neurodegenerative diseases, as ALS, cause progressive loss of motor function in upper limbs. Motor involvement, also affecting speech at some stage of disease, cause increasing difficulties in accessing to computer devices (and internet tools) that allow communication with caregivers, and healthy professionals. Thus, monitoring progression is important to anticipate new assistive technologies (AT), e.g. computer interface. We present a novel methodology to monitor upper limb typing task functional effectiveness. In our approach, an accelerometer is placed on the index finger allows to measure the number of keystrokes per minute. We developed algorithm that was accurate when tested in three ALS patients and in three control subjects. This method to evaluate communication performance explores the quantification of movement as an early predictor of progression.

1 INTRODUCTION

Quantitative assessment of the motor performance of human body has raised important questions and scientific findings in last decades. Modern technology allows to study movement using miniaturized and wearable equipment. Namely, accelerometers used as clinical tools, are broadly used to monitor daily activity and tremor, specially in movement disorders (Bonato, 2003; Godfrey et al, 2008). In context of progressive diseases, monitoring tools that can be used in the daily living are important to track progression and adjust treatments and interventions (Shany et al, 2012; Bustamante et al, 2011).

The use of computer devices as assistive technologies (ATs) for Communication is very important concerning quality of life in some neuromuscular diseases that affect speech or writing abilities. Particularly in Amyotrophic Lateral Sclerosis (ALS/MND), patients experiment progressive loss of speech and limbs motor function and consequent difficulties in communicating without ATs (Korner et al, 2013; Beukelman et al, 2000). Access to computer devices is also important to give access to eHealth services for patients.

Although speech progression in ALS has been studied for the purpose of monitoring communication needs (Ball et al, 2002), writing function (as upper limb motor progression) has been underestimated as a variable for monitoring communication abilities of ALS patients. ATs for communication are commonly based on electronic devices and typing tasks (considering the use of text-to-speech technologies), either on a physical keyboard or a virtual keyboard accessed via touchscreen. Due to the neurodegenerative characteristics, it is important to follow symptoms of progression in upper limb motor control to identify periods to adapt or introduce ATs, aiming at augmenting users' functionality in communication (Beukelman, 2011; Bongioanni, 2012).

In this study, we aim to investigate the potential of monitoring progression of upper limb motor functionality needed to perform typing tasks on a keyboard. For this purpose, we captured data from a 3D accelerometer placed on the index finger (finger

used to press the keys) and captured a 10-word typing task. In this paper, we describe the methodology and the developed algorithm to detect and quantify keystrokes events from accelerometer signals captured during the experiments. As first results, we present data from three ALS patients and from three control subjects (with no diagnosed neurological disease).

The rest of the paper is organized as follows: Section 2 describes methodology used to acquire data from accelerometer; Section 3 describes the proposed algorithm for typing detection; in Sections 4 results from data analysis are presented; Section 5 and 6 present discussion and main conclusions on the first results of this study.

2 METHODS

2.1 Participants

We present results from 3 patients with ALS and 3 healthy control subjects. ALS patients (2 women and 1 man) had a mean age of 53 years old (37, 59 and 63 years old). At baseline assessment, all participants with ALS had clinical evaluation of ALSFRS-r (Cedarbaum et al, 1999) speech subscore less or equal to 2, though all were able to use upper limbs to type on a keyboard. Patients had no dementia. Healthy control subjects (2 women and 1 man) had mean age of 32 (23, 35 and 37) years old.

2.2 Equipment

For accelerometry acquisition a BiopluxResearch system (PLUX SA) was used. In our research settings, we used the system with a 3-axial MEMS accelerometer sensor *(*±3g measurement range). Sensor was placed in exterior part of index finger of the functional hand, as depicted in Fig.1. The three axes were measured according to Fig.1 in directions: anterior-posterior(X), distal(Y) and lateral(Z). Data was sampled at 1KHz. Data was acquired via Bluetooth to a laptop computer to be later processed using *Python* tools. A second laptop was used by the participants to perform the typing tasks.

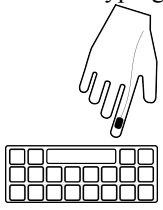

Figure 1: Index finger for typing.

2.2 Procedure

Subjects were asked to type a 10-word sentence using just the index finger. Accelerometer was placed in the finger and data from the accelerometer was saved. The same accelerometer sensor was always used. Patients were evaluated in 3 sessions, in 3 months intervals. Control subjects just performed one trial in one session, as no progression is expected for control participants. A camera was also used to capture typing task, for results validation.

Figure 2: Photo from an evaluation.

2.2.1 Outcome measures based on accelerometer

For simplification, we used Y axis (distal movements of index finger) to characterize typing function, as this is the direction related to the movement of pressing keys (as illustrated in Fig 1). As outcome variables we wanted to have *number of keystrokes*, *typing rate*, *time between keystrokes*, *time duration of each keystroke*, *amplitude of acceleration signal (*amplitude of acceleration of finger movements in distal direction), *magnitude of acceleration signal (*calculated as the Euclidean vector for the 3-axis acceleration signal).

2.3 Algorithm for typing detection

We analysed accelerometer signals from patients and control subjects. Key types from the 10-word sentence were analysed. Fig.3 shows the plot from the acceleration signal of one of the control subjects, illustrating a set of keystrokes and one isolated keystroke.

An algorithm was developed to extract outcome variables from each typing task.

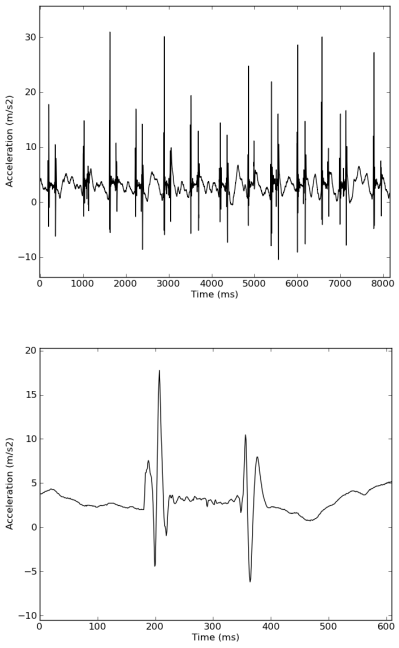

Figure 3: Plots from keytyping from a control subject. (up) Set of 13 keystrokes (down) One keystroke: first acceleration pulses correspond to press action and the second acceleration pulses correspond to release action.

2.2 Characterization of a *typing* action

For the setup suggested in this paper, a keystroke (for simplicity, we consider signal from Y-Axis to analyze movements in distal direction) is characterized by two *events* of acceleration (Figure 3). The first *event* is related to pressing action and the second *event* is related to releasing action.

2.2.1 Signal processing for detection of typing actions

Proposed algorithm first removes DC component from acquired data, then uses a moving average algorithm to smooth the signal's module (Figure 4). From the processed signal, peaks are detected (from a threshold value calculated as a factor of maximum amplitude) as events of pressing and releasing keys – each group of two near peaks corresponds to the signal of a keystroke.

Due to erroneous movements (from video analysis we could identify hand gestures performed during typing task or touching a key with no pressing action) two kinds of peaks were detected as frequent false typing events:

- isolated event: isolated peaks or a peak close to a pressing event (video analyses show that a single peak may occur when user touches a key but doesn't press it – this is caused by a hesitation (commonly caused by low experience in the use of a qwerty keyboard);
- third event: we could observe in the acquired signals frequent low amplitude acceleration impulses prior to a typical keystroke signal. From the video analysis we could conclude that these acceleration impulses are due to slow typing (an evident delay between touching the key and pressing it).

To guarantee a pair number of peaks (press/release keys), previously described false typing events were removed: signal was analysed near each detected peak of acceleration. Isolated events were eliminated and, in groups with more than two close events, only the two with higher amplitude values were kept.

Keystroke events detected with the proposed algorithm are depicted in Fig 5.

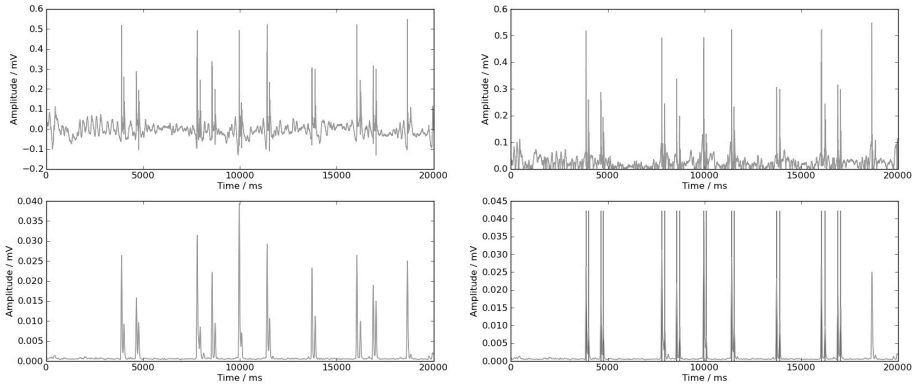

Figure 4: (top left) raw signal; (top right) signal's module; (bottom left) filtered signal using smooth algorithm; (bottom right) bottom left signal and vertical lines representing peaks detection. All schematic representations are of 20s of samples from one patient performing a typing task.

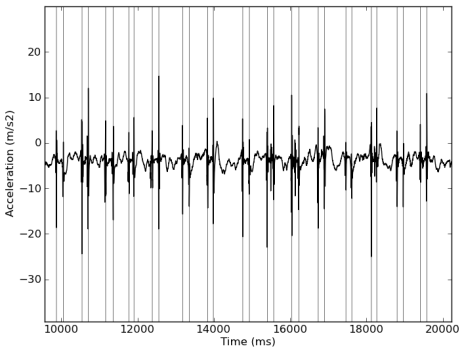

Figure 5: Representation of keystrokes detected from approximately 10s of accelerometer signal acquisition (a patient performs 15 keystrokes, typing a 10-word sentence).

2 RESULTS

All collected signals were processed with the proposed algorithm. Features from typing task were calculated and are represented in Table 1. We also measured performance of typing task, presented in second column of Table 1 as *words per minute* (wpm), using visual video analysis.

We applied the algorithm to the signals of control subjects and patients (different users and three different periods during disease progression).

As can be observed in Table 1, in spite all subjects were asked to do the same typing task, the number of keystrokes performed in each typing task (#ks) is not always the same. This is due to variability among subjects experience. For example, some of the patients forgot to add spaces between two different words, some added more than one space or used the backspace to correct a mistake. One of the patients (patient P1, in Table 1) had no experience in using computer devices, the reason why we reduced the sentence to 5 words (half of the sentence). In fact, as it is not the aim of this study to evaluate the written text, participants had no specific constraints (related to text) when performing the typing task.

From visual observation of accelerometer plots, a validation of the algorithm was performed, based on a manual adjustment of the algorithm variables (i.e. threshold value for peak detection and time window to search for false events). Number of keystrokes detected by the algorithm was confirmed with the number counted in video observation. Results are presented in Table 1. We calculated a Pearson correlation of 0.98484 between *words per minute* (obtained from video analysis) and *keyrate* (result of proposed algorithm from accelerometer analysis) for the set of all analyzed data. These results validate the used methodology to performance evaluation.

3 DISCUSSION

Finding methodologies that can early predict progression allows a faster and customized response of interventions and care. We hypothesized there is a relation between user performance on typing tasks (measured as communication speed - *wpm*) and respective kinematic analysis of typing and that this can provide a more sensitive tool to detect progression in upperlimbs motor function. A methodology to collect data from a 3-axis accelerometer placed on the index finger was developed for typing task.

A set of data captured from healthy subjects and ALS patients (in different time periods) was analyzed. Presented results show that keystrokes detected from the developed algorithm had high correlation with performance measured by video analysis. Although, high accuracy was due to fine adjustment of two parameters, which had to be manually adjusted for each data set. It was not possible to establish a peak threshold common to all studied signals – it had to be manually adjusted within different users or along different samples from the same user. Also, using the suggested algorithm, it was difficult to distinguish very low amplitude peak from noise or involuntary movement – window size to remove false events had to be manually adjusted for each sample.

From a preliminary analysis of the results presented in this paper, we could observe that, for ALS patients, in spite performance values in different periods of evaluation are variable (we can't always find evident decrease in time), the maximum amplitude of y-axis signal ($V_Y$máx, Table 1) and the mean value of the amplitude of magnitude signal (last column in Table 1) always decrease along the different time periods of evaluation (3 months interval, approximately). Although careful analysis is part of future work for the presented study, these preliminary results suggest a new surrogate marker of typing function deterioration, potentially more accurate than simple typing performance observation.

4 CONCLUSIONS

In this paper we present an algorithm for studying typing performance through accelerometry.

Table 1: Results from the analysis of acquired data with the algorithm proposed for typing detection. Each row describes the results from control subjects (C_i) and patients (P_i) in the different evaluation times (T_i). #ks – number of keystrokes; µ tbt_key – average of time interval between keystrokes; µ tkey – average time duration of keystrokes; VYmáx – maximum amplitude of Y-axis of accelerometer signal; Magn. Máx – maximum amplitude of magnitude of accelerometer signal; Magn.Mean – mean magnitude of the accelerometer signal).

Particip.	wpm (video)	keyrate	# ks	total time (s)	µ tbt_key	µ tkey	$V_Y$máx (mV)	Magn. Máx (mV)	Magn. Mean µV
C1	10	43	43	60	331.8	75	623.79	220.12	60.99
C2	10	44	44	60	852.1	244	253.44	151.91	32.65
C3	10	44	44	60	1011.4	144.5	299.53	192.05	31.18
P1.T0	3.04	13.17	18	82	3952.2	255.1	623.43	149.26	40.68
P1.T1	3.1	11.46	17	89	4819.4	186.6	555.29	314.36	33.6
P1.T2	3.87	12.00	13	65	4129	241.5	412.22	195	31.44
P2.T0	16.66	67.89	43	38	527.6	168.1	624.19	147.34	38.34
P2.T1	16.61	62.67	47	45	669.9	188.5	475.47	225.08	36.62
P2.T2	17.3	61.82	44	42.7	666.1	252.5	427.32	129.08	33.72
P3.T0	7.69	28.53	39	82	1282.3	712.8	495.77	212.19	42.64
P3.T1	9.38	33.75	45	80	736.3	847.1	480.26	177.54	32.35

A 3-axis accelerometer was placed in the index finger of 6 participants (3 with progressive neuromuscular disease and 3 healthy participants). Signal processing of the accelerometer signals showed high correlation between independent measures of performance: words per minute (from video analysis) and keystrokes per minute (from accelerometer).

Presented algorithm should be improved to automatically adjust all the parameters for different users and different stages of progressive disease. As future work, a detailed analysis of other parameters of accelerometry, independent from performance measures, should be done.

REFERENCES

Ball, L.J., Beukelman, D.R. and Pattee, G.L., 2002. Timing of speech deterioration in people with amyotrophic lateral sclerosis, *Journal of Medical Speech-Language Pathology*, 10(4), 231–235.

Beukelman, D., Fager, S. and Nordness, A., 2011. Communication Support for People with ALS. In *Neurology Research International*, Article ID 714693.

Beukelman, D.R., Yorkston, K.M., Reichle, J., 2000. *Augmentative and Alternative Communication for Adults with Acquired Neurologic Disorders.* Brookes H. Paul Publishing, Baltimore.

Bonato, P., 2003. Wearable sensors/systems and their impact on biomedical engineering. In *IEEE Engineering in Medicine and Biology Magazine*, 22(3), 18–20.

Bongioanni, P., 2012. Communication Impairment in ALS Patients: Assessment and Treatment. In Maurer, M. (Ed.) *Amyotrophic Lateral Sclerosis*. Available from: http://www.intechopen.com/books/amyotrophic-lateral-sclerosis

Bustamante, P., Solas, G. and Grandez, K., 2011. Neurodegenerative Disease Monitoring Using a Portable Wireless Sensor Device. In Chang, R. (Ed) *Neurodegenerative Diseases - Processes, Prevention, Protection and Monitoring*, InTech Publisher. Available from: http://www.intechopen.com/books/neurodegenerative-diseases-processes-prevention-protection-and-monitoring

Cedarbaum, J.M., Stambler, N., Malta, E., Fuller, C., Hilt, D., Thurmond, B., Nakanishi. A., 1999. The ALSFRS-R: a revised ALS functional rating scale that incorporates assessments of respiratory function.

BDNF ALS Study Group (Phase III). In *Journal of the Neurological Sciences,*169(1-2),13-21.

Godfrey, A., Conway, R., Meagher, D. and ÓLaighin, G., 2008. Direct measurement of human movement by accelerometry, In *Medical Engineering & Physics*, 30, 1364–1386.

Korner, S., Siniawski, M., Kollowe, K., Rath, K.J., Krampfl, K., Zapf, A., Dengler, R., Petri, S., 2013. Speech therapy and communication device: Impact on quality of life and mood in patients with amyotrophic lateral sclerosis. In *Amyotrophic Lateral Sclerosis and Frontotemporal Degeneration*, 14, 20–25.

Shany, T., Redmond, S. J., Narayanan, M. R. and Lovell, N. H., 2012. Sensors based wearable systems for monitoring of human movement and falls. In *IEEE Sensors Journal*, 12(3), 658–670.

Coherence and Phase Locking Disruption in Electromyograms of Patients with Amyotrophic Lateral Sclerosis

Mafalda Camara[1], Mamede de Carvalho[3], Tiago Araújo [1,2]Carla Quintão[1], Hugo Gamboa[1,2]
[1]*Faculdade de Ciências e Tecnologia, Universidade Nova de Lisboa*
[2]*PLUX - Wireless Biosignals, Lisboa, Portugal*
[3]*Instituto de Medicina Molecular, Faculty of Medicine, University of Lisbon, Lisbon, Portugal*
m.camara@campus.fct.unl.pt, mamedemg@netcabo.pt, tsergio@plux.info, cmquintao@fct.unl.pt, hgamboa@plux.info

Keywords: Contra and Ipsilateral, Coherence, Beta Band, Phase Locking Factor (PLF), Amyotrophic Lateral Sclerosis (ALS), Electromyography (EMG).

Abstract: In motor neuron disease, the aim of therapy is to prevent or slow neuronal degeneration and early diagnosis is thus essential. Hypothesising that beta band (15−30 Hz) is a measure of pathways integrity as shown in literature, coherence and PLF could be used as an electrophysiological indicator of upper and lower neuron integrity in patients with ALS. Before further analysis, synthetic EMG signals were computed to verify the veracity of the used algorithm. Coherence and PLF analysis were performed for instants of steady contraction from contra and ipsilateral acquisitions. Ipsilateral acquisitions were performed for one member of each group and results present significant differences between both groups. Contrarily, contralateral acquisitions were performed on 6 members of each group and results present no significant differences. PLF analysis were computed for ipsilateral acquisitions and, similarly to coherence, results show significant differences between both groups. PLF was also analyzed for contralateral acquisitions, and results show no significant differences within groups, as expected since no coherence was found for the same acquisitions. So, while control subjects present no neuronal or muscular problems and therefore higher synchrony and coherence for beta band, patients with ALS do not present synchronism and coherence in any frequency, specially for beta band. All results allowed to conclude that contralateral coherence is not a good measure of corticospinal pathways integrity. However, ipsilateral acquisitions show promising results and it is possible to affirm that ipsilateral measurements may reflect neuronal degeneration. For future work is suggested a deeper analysis of PLF, that appear to have potential as a quantitative test of upper and lower neuron integrity related to ALS.

1 INTRODUCTION

ALS, one of the major neurodegenerative diseases, is a progressive incurable motor neuron disorder fatal in all cases. Associated therapy involves slowing down or even preventing neuronal degeneration, that requires strategies for early diagnosis and/or treatment. As a general rule, patients with ALS are diagnosed when there is already extensive motor neuron degeneration present, since the diagnosis is hampered by the impossibility to access the corticospinal tract. Some motor cortex cells are capable of synchronizing their discharge with local oscillations in a 15−30 Hz range of frequency - beta band. This synchronism happens during rest or steady contraction but is not common during movement. Despite all the research on this subject, there is no agreement on which function might induce such periodic activity (Baker et al., 2006). Some oscillatory cortical activity involves pyramidal neurones and is reflected in the descending drive to the muscles, being distributed to agonist and antagonist muscles, which can be observed in the EMG of these muscle pairs through coherence in beta band (Cordivari et al., 2002). Corticomuscular coherence measures contributions from both ascending and descending pathways, which was proved by phase analysis, suggest that muscles led the cortical recordings (de Carvalho, 2012). The timing of synchronism is dependent on the intrinsic properties of the inhibitory interneurons and their conduction delay (Jackson et al., 2004). In both upper and down motor neuron disease, the focus is to prevent, if possible, or slow neuronal degeneration. Based on the hypothesize that beta band coherence could be used as an indicator of neuronal integrity, the aim in this work was to obtain coherence values averaged for each popu-

lation and if significant differences were present between them, to find a way of an early diagnose for ALS resorting to contra lateral acquisitions.

1.1 ALS

ALS is one of the major neurodegenerative diseases, a progressive disorder that involves widespread degeneration of the motor system neurons from the destruction of layer V pyramidal neurons from the motor cortex to the anterior horn of the spinal cord. To diagnose such a disease it is necessary to find upper and lower motor neuron degeneration in multiple regions: bulbar, cervical, thoracic and lumbar. This disorder is characterized by the neurological regions affected, but there are common features observed in all patients such as a rapidly progressive weakness, muscle atrophy, muscle cramps, fasciculations, muscle spasticity, difficulties in breathing (dysponea), difficulties in swallowing (dysphagia) and difficulties in speaking (dysarthria). Patients tend to lose their abilities to control voluntary movements and symptoms tend to greatly reduce their quality of life (Kiernan et al., 2011).

1.2 EMG and Beta band

Voluntary movement is associated with the presence of rhythmic activity in motor cortex. Beta band, comprising a range of frequencies from 15 to 30 Hz, appears to vary its magnitude prior and during voluntary movements and are associated with the attempt to perform certain tasks (Halliday et al., 1998). In this same frequency band, cortical activity and motor unit firing are correlated during sustained voluntary contractions. Intermuscular coherence (EMG - EMG) between different muscle groups appears to detect characteristics of the same rhythmic processes suggesting a common drive from corticospinal pathways. The precise function and genesis of these same cortical oscillations still remains elusive (Marsden et al., 2000). Motor units from muscle pairs can be modulated by a descending 15 -30 Hz drive, demonstrating that this drive is mediated via corticospinal pathways, that oscillations within this band occur in the sensorimotor cortex which are coherent with muscles (Marsden et al., 2000; Nishimura et al., 2009). These oscillations may arise in motor systems in order to promote synchronous neuronal firing between neurons populations that are spatially distributed but functionally related, providing means of linking different neuronal populations (Marsden et al., 2000). Coherent activity may represent a common element in coding activity in simultaneous active motor centres. Cortical areas involved in the same motor task may be coherent with each other. Active muscles show coherence around beta band, reflecting the activity of neuronal structures involved in driving the spinal motoneurons (Nishimura et al., 2009). Coherence has demonstrated that some of these oscillations are probably transmitted via the pyramidal tract to activate muscles and may induce the same rhythm in them (Nishimura et al., 2009).

1.3 Coherence

Coherence analysis of motor unit firing behaviour can provide information about the organization of networks responsible for driving spinal motoneurons during task performance and assess common presynaptic inputs that synchronize motor units populations (Hansen et al., 2005). In the human body, different activities may be characterized by functional activities in distinct circuits, due to muscles discharges at a certain frequency by central nervous system (CNS). Some of these oscillating frequencies let to spinal motoneurones (Grosse et al., 2002). Coherence is performed using discrete Fourier transforms, so the parameter nonequispaced fast Fourier transform (NFFT), that represents the number of data points used in each block must be defined. For the rectified x and y signals, auto spectra $f_{x,x}(\lambda)$, $f_{y,y}(\lambda)$ and cross spectra $f_{x,y}(\lambda)$ are calculated to assess measures of correlation (Farmer et al., 2007; Grosse et al., 2004). As a function of frequency, cross-correlation is assessed by coherence function - $|R_{x,y}(\lambda)|^2$ - defined as the squared magnitude of cross spectrum, normalized by the product of the two auto spectra as show in equation 1.

$$|R_{x,y}(\lambda)|^2 = \frac{|f_{x,y}(\lambda)|^2}{f_{x,x}(\lambda) f_{y,y}(\lambda)} \tag{1}$$

Coherence analysis present frequency related values between 0, when signals are linearly independent from each other, and 1 for signals dependent linearly on each other, for the specific value of frequency. Results of coherence analysis are represented using pooled analysis for each population and compared within them.

1.4 PLF

During oscillatory activity, neurons fire synchronously. Therefore, common target cells will receive neural activity synchronously and so, oscillations play an important role for the timing of neural activity (Klimesch et al., 2008). On the assumption that coherence exists for beta band between two

signals, both signals must be synchronized within each other for these frequencies. So, the frequencies of interest are isolated by applying to the signal a band-pass filter at a narrow band centred at each frequency. From the obtained oscillatory signal, phase can be defined in the complex unit circle for each point data. The method used is based on the Hilbert transforms of the data. For signals x and y, $\phi_x(t)$ and $\phi_y(t)$ represent signals phase dependency on time, respectively, for $t = 1,...,T$. PLF between both signals is defined by (Almeida et al., 2011):

$$\rho_{xy} \equiv |\frac{1}{T}\sum_{t=1}^{T} e^{i[\phi_{jx}(t)-\phi_y(t)]}| = |\langle e^{i[\phi_x(t)-\phi_y(t)]}\rangle| \quad (2)$$

PLF assumes values from 0 to 1. 0 stands for signals entirely asynchronous, with phases randomly distributed; 1 stands for signals perfectly synchronized and with a constant phase lag. Values between 0 and 1 represent partial synchrony. PLF on this work is only calculated between two signals, specifically for all instants of steady contraction, where oscillations are expected. Results of PLF analysis are represented using pooled analysis for each population and compared within them.

2 ACQUISITIONS

2.1 Subjects

Focussing on previous published results, ipsilateral measurements were performed on 1 member from the group of patients and 1 member from the group of control. Contralateral measurements required the existence of two different groups of subjects: group of 6 patients presenting ALS and a control group of 6 subjects. All participants from the control group do not present any known neuronal or muscular disease, whereas patients with ALS had been diagnosed within less than one year. For patients with ALS that were in a more advanced stage of the disease, presenting more difficulties that limited their own movement control, it was impossible to collect an analysable EMG signal.

2.2 Recordings

For each ipsilateral acquisition, 4 signals were simultaneously acquired from each subject using EMG sensors attached to a bioPlux device. As observed in figure 1, besides the contra-lateral acquisition (as shown in figure 2), ipsilateral was simultaneously acquired. For both right and left hand, signals were collected using two sensors attached to first dorsal interosseus muscle; for both right and left forearm, signals were collected using two sensors attached to extensor digitorum communis muscle. Ground was placed in ulna bone inferior extremity, where no muscle activity is present.

Figure 1: Ipsilateral acquisitions experimental setup for left member: Bioplux research device, placement of two EMG sensors and ground.

For each contralateral measurement, two signals were simultaneously acquired from each subject using two EMG sensors attached to a bioPlux device. Each sensor (one for each hand) has 2 connected electrodes placed in first dorsal interosseus muscle. Ground was placed as in ipsilateral recordings. Surface electrodes placements are shown in figure 2.

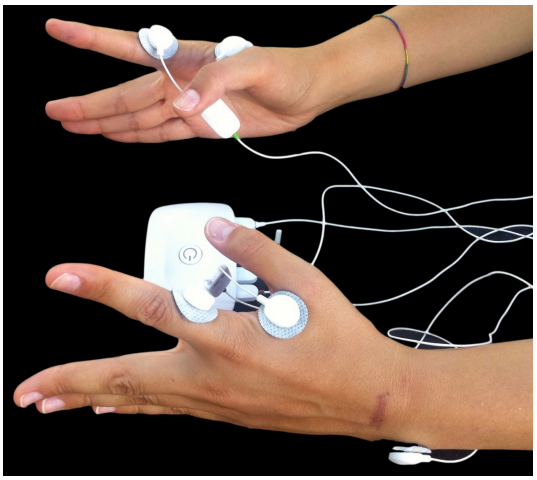

Figure 2: Contralateral acquisitions experimental setup: Bioplux research device, placement of two EMG sensors and ground.

EMG signals are recorded using bioPLUXresearch unit. This device collects real time biosignals at a frequency rate of 5 KHz and EMG sensors have second order band pass filter with *cutoff* frequencies of 25 and 450. Data is transmitted via bluetooth to a computer, where the signals can be saved and visualized.

2.3 Acquisition Protocol

Subjects were asked to seat and place both hands on a desk, 10 cm away from each other in a parallel position and with hand palms facing each other in 90 degrees of flexion with the elbow. Subjects had to elevate both index fingers vertically with a maximum articular amplitude in a direction opposite to the other fingers position, hold that position for 3 seconds while maintaining a certain force/pressure and then return to the initial position, where it remains for 3 seconds while relaxing as much as possible. This movement was repeated for 5 minutes or less according to maximum time tolerated by the patients. The coordinated movement was guided by a programmed sound and both fingers had to be as much coordinated as possible one to another. The protocol was used for both contra and ipsilateral acquisitions.

3 Signal Processing

The acquired signals were processed using Python language. Signals were filtered by a third order Butterworth band pass filter of $30-2000$ Hz. In order to extract information about coherence and PLF, intervals of contraction common to both signals had to be isolated from intervals of relaxation, since coherence is better estimated during periods of steady contraction (Fisher et al., 2012). Signals presenting higher amount of noise will conceal real information, inhibiting to distinguished contractions from relaxation intervals so predictably. This and the differences among individual signals, does not allow to predefine an onset value common to all signals. So, instead of using a method based on the EMG signal envelope, a method based on statistical model was used to define EMG onset. Initially, more than one value was assigned to both on and offset for each contraction given that EMG signals oscillate. In order to obtain the correct on and offset for each contraction, the excessive ones were removed when: (1) the number of samples between the on and offset is too short or (2) when the number of samples between the off and following onset is too short. To guarantee that these signals have commons intervals of contractions, it is chosen, for each contraction, the highest value from both onsets and the lowest from both offsets.

3.1 Coherence Processing

Using two long common sections of data from an interval of one contraction, coherence is calculated using, power spectral density (PSD) calculus for each section and Cross power spectral density (CSD) between both signals sections. All EMG signals, with the purpose of coherence calculus, were full-wave rectified before any fast Fourier transform (FFT) was calculated. Sampling frequency is placed as 5 KHz, the NFFT as 2048, and the value that dictates the dependency between FFT windows is half of NFFT value. Coherence is reported in two different ways. First, to provide a visual representation of coherence dependency on frequency (in the imaginary domain), coherence mean values among intervals of contraction for a given muscle pair was performed across all patients within a group of subjects; this allows to precise coherence for each patient acquisition based on averaging multiple independent instants of data. Second, to provide an estimation of coherence dependency on frequency across the population of each group, mean coherence was calculated for the same values of frequency for a given muscle pair among all subjects within the same group. To assure that the wanted band of frequency was present in both signals of each patient, frequency spectrums were computed for all instants of contraction and then averaged to present an individual spectrum for each patient.

3.2 PLF Processing

Since the beta band frequencies are been studied, PLF was calculated for specific values of frequency f within this same band $[15,30]$ Hz with a resolution of 1 Hz. This procedure was performed among both control and patient groups. Each signal was band pass filtered ($[f-2, f+2]$), f being the analyzed frequency, to eliminate from the signal all off the other undesirable frequencies. Instants of contraction where again isolated and for each, PLF calculated between each pair of contra-lateral measurements. Since is among instants of steady contraction that coherence is better estimated, PLF analysis was also performed for these same instants. To present a final value for each member of each group, PLF was averaged between all contractions within the same acquisition. This procedure, is performed as many times as the number of frequencies that are to be studied. PLF was averaged among all members within the same group to present a PLF value, dependent on frequency choice, for a population.

4 DISCUSSION

4.1 Synthetic EMG

For validation of the algorithms, synthetic EMG signals were used to compute coherence. To prove that coherence exists between two signals linearly dependent on each other for particular values of frequency, sets of signals were constructed and defined by the following equation:

$$signal = (sin(t \times 2\pi f) + k) \times n(t) \times mod(t) \quad (3)$$

where t is a sequence of integer numbers, incremented by one unit, with a desirable length; t is referred in seconds by dividing the desirable length for 5000, to take into account the sampling frequency. $n(t)$ is a Gaussian noise ($\mu = 0$ and $\sigma = 1$), k the signal envelope, f the signal's frequency and the portion $mod(t)$ represents the rest of the division of t by 6 bigger then 3 - guaranteeing instants of contraction and relaxation of 3000 ms.

An example with $t = 100.000$ and $k = 3$ is shown in figure 3.

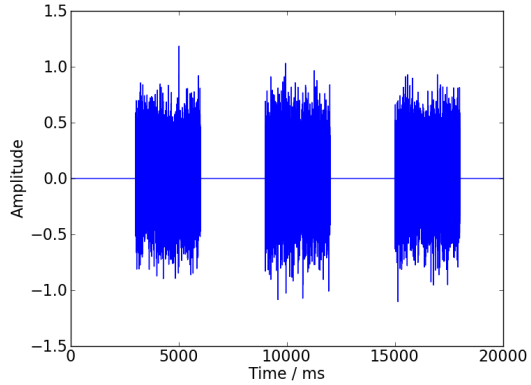

Figure 3: Schematic representation of the signal defined by equation 3.

Multiples signals were created, choosing t : 4×10^4, 4×10^6 or 1.955×10^6 samples and f : 10, 20 or 40 Hz. Number of samples were chosen to provide signals with 1, 13 and 65 instants of contractions to decide the time sampling for acquisitions; frequency values were chosen taken into account that beta band is being studied. For all created signals, coherence was calculated between two signals of the same kind (simulating both right and left hand). Coherence defined by equation 3 is performed for instants of contraction and then averaged for the entire measurement. Coherence results do not present any dependency on the choice of f value, since it assumes 1 for that same frequency and near to 0 for the remaining. On the contrary, coherence results seem to depend on the choice of signals length. Two types of signals were performed, both defined by equation 3, with common value of 40 Hz for f but with different value of t. First, signals with 65 instants of contraction, and second signals with 1 instant of contraction; two sets of signals, with different portions of $n(t)$, were created to test coherence between them.

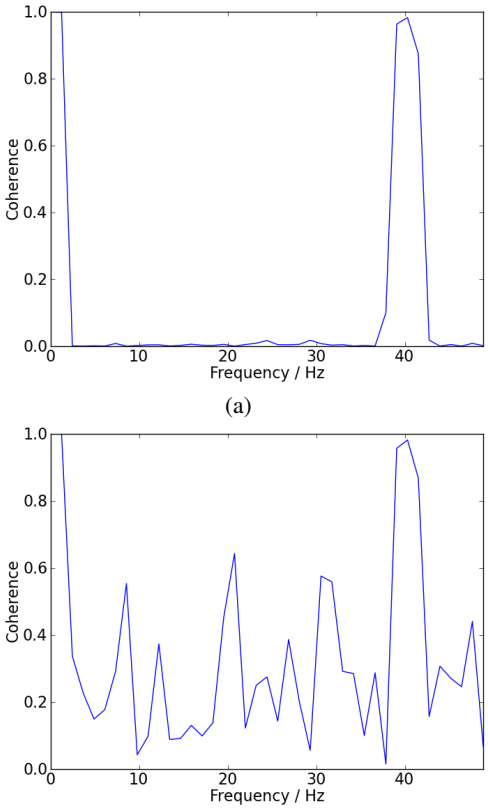

(a)

(b)

Figure 4: (a) Coherence values between two similar signals with 1.955×10^6 samples. (b) Coherence values between two similar signals with 4.0×10^4 samples. Both signals are defined with f as 40 Hz.

Results of mean coherence for these pair of signals can be observed in figure 4 and it is possible to affirm that the higher the signals length, the more accurate are the coherence results. It is possible to observe that in figure 4(b) coherence is different than 0; but the same phenomenon does not happen in figure 4(a). So, averaging coherence for greater amount of instants of contraction, appears to reduce the coherence detected in frequencies derived from the presence of noise (figure 4(b)), that only tends to disappear when not found among other contractions. Therefore, the use of long acquisitions increases the precision of coherence.

4.2 Coherence Analysis

4.2.1 Ipsilateral

For both signals collected, ipsilateral coherence was analyzed for instants of contraction using NFFT as 4096. Graphical representation, for each patient, is shown in figure 5.

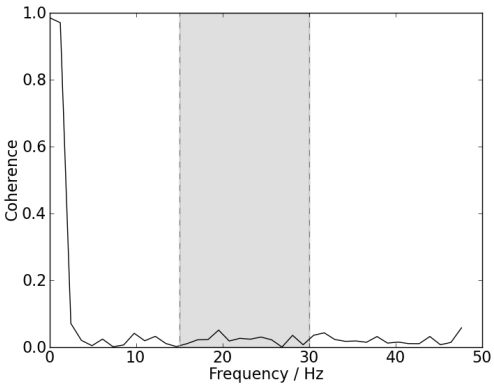

(a)

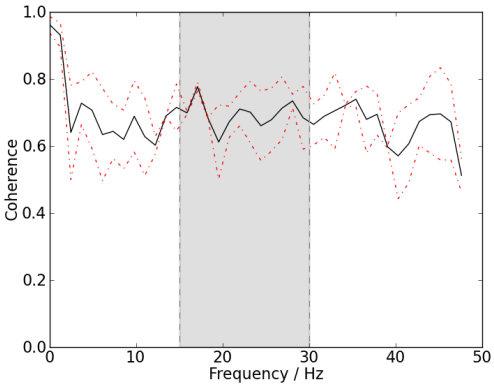

(b)

Figure 5: (a) Ipsilateral coherence acquired from a patient. (b) Ipsilateral coherence acquired from a control subject. Delimited by the grey box, are represented the frequencies corresponding to beta band.

Analysing results, it is possible to observe that the signal acquired from the patient presents coherence near 0 for all frequencies, while coherence from the control subject presents high values for most presented frequencies, despite the fact that beta band is not distinguished from the remaining frequencies. Differences are significant since for beta band, coherence mean value for the patient was 0.0235 ± 0.0127 and for the control subject 0.6936 ± 0.0401. Patient results would be expected since coherence in beta band is not visible for ALS. On the other hand, results from the control group are not expected since results do not appear to be any close from those observed in literature, but significantly higher than those observed for patients; differences in results may be explained by differences in acquisition protocol, used algorithm or parameters.

4.2.2 Contralateral

Prior to coherence analysis, the presence of beta band frequencies among all signals was tested, recurring to frequency spectrums analysis. Instants of muscular contraction were isolated, its frequency spectrum for full-wave rectified instants, for a variable NFFT value, and averaged within all contractions to present a result for each measurement; these frequency spectrums were performed by PSD calculus. Graphical representations of these results for patients group are shown in figure 6(a), and for control group in figure 6(b), for NFFT as 2048.

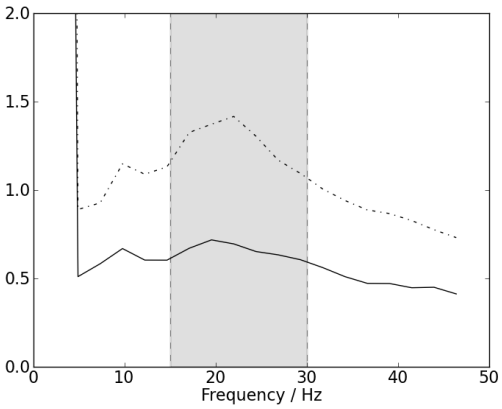

(a)

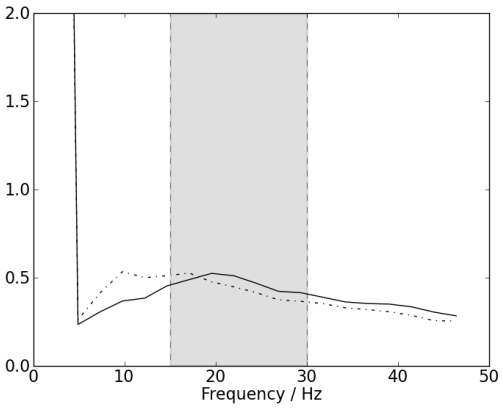

(b)

Figure 6: Schematic representation of frequency intensity dependency. Results collected from the left hand are represent by the dotted line and results collected from the right hand are represent by the straight line; delimited by the grey box, are represented the frequencies corresponding to beta band. (a) Results for the group of control and (b) for the group of patients.

In figure 6, results show a higher presence of beta band frequencies, since they appear more enhanced than the remaining, for the majority of all results from both hands and groups. When on instants of contraction is calculated a frequency spectrum and within the same group averaged, it can be concluded that beta band is present among signals and it is reasonable to expect coherence existence. As shown in 4.2 , ipsilateral coherence is a precise indicator of neuronal degeneration development. Contralateral coherence is tested to check whether results are similar to those obtained for ipsilateral acquisitions. Contralateral coherence between both interosseous muscles, one from each side, are shown for patients and control subjects groups in figures 7(a) and 7(b), respectively. Results of coherence dependency on frequency for both groups using NFFT as 2048 are summarized in figure 7.

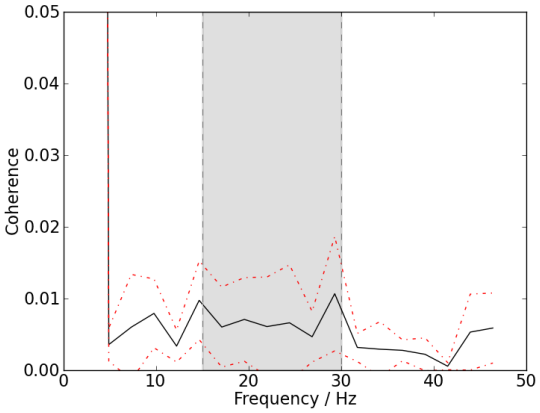

(a)

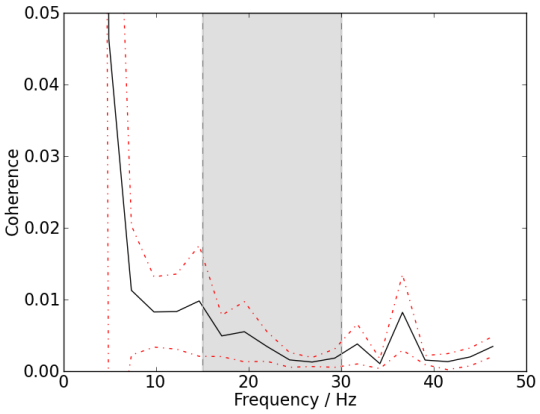

(b)

Figure 7: Schematic representation of mean coherence dependency on frequency by the straight line and it's standard deviation by the dotted line, with NFFT placed at 2048; delimited by the grey box, are represented the frequencies corresponding to beta band. (a) Results from the group of patients. (b) Results from the control group.

Results from the group of subjects is not entirely similar to those observed in literature. Coherence for the beta band frequencies does not stand out from the presented in the remaining frequencies. There was no significant intermuscular coherence present for any of the acquisitions from the group of subjects, since for beta band, pooled coherence value for the patients group was 0.0069 ± 0.0019 and for the control group 0.0031 ± 0.0017. Coherence was present within significance (in the same order of magnitude found in literature), but not higher on the beta band than the remaining for other frequencies. The analysis from the group of patients shows a behaviour similar with the group of patients. Contralateral coherence between coactivated muscles from left and right side is not considered significant within the beta band. Therefore, despite the possible presence of these frequencies (beta band) on both signals, they do not significantly depend linearly from each other.

4.3 PLF Analysis

4.3.1 Ipsilateral

To present a final value for each member of each group, PLF was averaged between all contractions within the same acquisition, for each value of frequency among beta band. Therefore, this procedure is performed as many times as the number of frequencies that are to be studied. PLF was averaged among all members within the same group to present pooled results, for ipsilateral measurements for both groups of subjects. The frequencies of interest and its respective PLF values are represented in figure 8.

In figure 8(a) is visible that results are similar to those obtained in 4.2.2. PLF values do not stand out from the remaining in beta band and do not assume significant values for any frequency. On the other hand, observing figure 8(b), PLF assumes much higher values and beta band frequencies appears to stand out from the remaining. Differences are significant since for beta band, PLF mean value for the patient was 0.1312 ± 0.0310 and for the control subject 0.6664 ± 0.0093. Contralateral analysis acquired simultaneously with ipsilateral, for coherence and PLF were also performed but results do not differ from those presented in 4.2.2 for both groups of subjects. Both results present low significant levels for both subjects and therefore are not relevant to be taken into deeper analysis or to be presented.

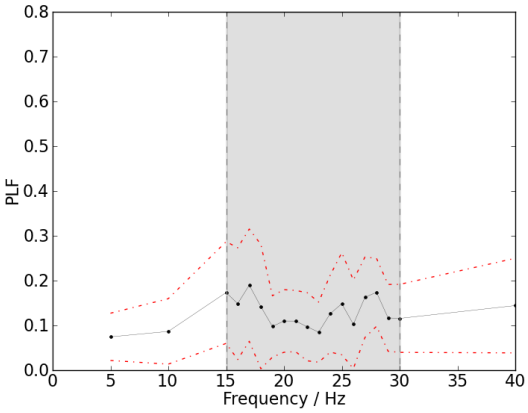

(a)

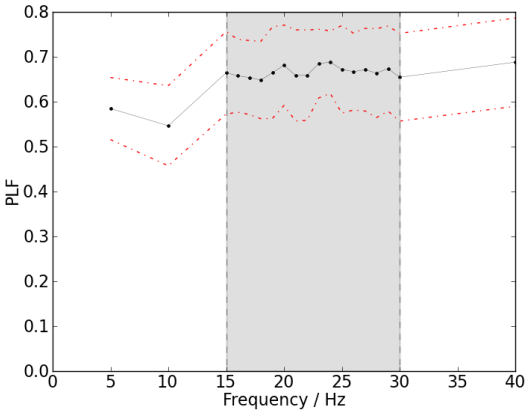

(b)

Figure 8: (a) Mean values of PLF for instants of contraction dependent on frequency, for the group of patients. (b) Mean values of PLF for instants of contraction dependent on frequency, for the group of control. Delimited by the grey box, are represented the frequencies corresponding to beta band. Results are present for ipsilateral acquisitions.

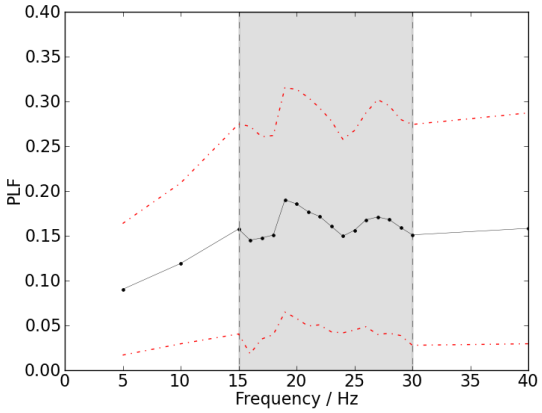

(a)

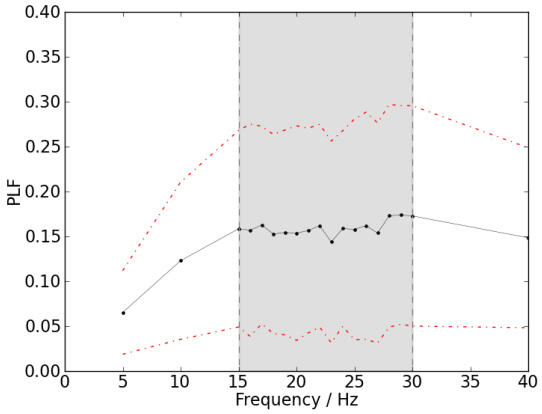

(b)

Figure 9: (a) Mean values of PLF for instants of contraction dependent on frequency, for the group of patients. (b) Mean values of PLF for instants of contraction dependent on frequency, for the group of control. Delimited by the grey box, are represented the frequencies corresponding to beta band. Results are present for contra lateral acquisitions.

4.3.2 Contralateral

Contralateral analysis are represented in figure 9, where mean values of PLF depending on frequency are visible, for the group of patients and of control in 9(a) and 9(b), respectively. As observed in both graphical representations of figure 9, PLF values do not significantly stand out for the beta band frequencies, since for beta band, PLF pooled value for the patients group was 0.1169 ± 0.0068 and for the control subject 0.1169 ± 0.0057.

5 CONCLUSIONS

Synthetic EMG signals with a specific known value of frequency were used to test coherence between two signals of the same type, to find whether coherence among them is present for that same frequency. For two signals of instants of contraction and relaxation with the same frequency, mean coherence between them for instants of contraction, are close to 1 for the specific frequency and near 0 for the remaining. So, varying signals frequency value does not change coherence general trends. But, altering these signals length, changes the number of instants of contraction used to present final averaged coherence, and the lower the number of samples, the higher will be the influence of noise. Both coherence and PLF analysis in ipsilateral acquisitions present sig-

nificant differences between both groups of patients, as already proved by previous publications. Results from the group of patients present no significant differences from the results obtained for contra lateral acquisitions but the group of subjects, presents higher values of PLF and coherence for all frequencies, especially for beta band. So, it is possible to assume that while control subjects present no neuronal or muscular anomalies and therefore higher synchrony for beta band, patients with ALS do not present synchrony in any frequency, specially for beta band. All results allow to conclude that ipsilateral analysis is a good measure of corticospinal pathways integrity. Frequency spectrums were performed for contra lateral acquisitions and it was demonstrated that beta band frequencies are present in instants of steady contraction. But, as proved by coherence and PLF analysis beta band frequencies in contralateral acquisitions was not present in neither for patients or control subjects. Neither differences or significance values were found for both control and patients. Therefore, it is to conclude that contra lateral frequency analysis is not a good marker for beta band frequencies studies. Comparing both methods used to study frequency domain, PLF analysis may be seen as a more practical method since it requires smaller sections of data, compared to coherence. On the other hand, PLF can only be analysed for a specific value of frequency, while coherence is analyzed for the range of frequencies presented on data. To conclude, as further work is suggested to rely on the possibility of using PLF analysis to observe beta band and assess about neuronal pathways integrity in ipsilateral acquisitions. Therefore, it seems possible that studying PLF serves as a method of diagnosing ALS.

REFERENCES

Almeida, M., Vigário, R., and Bioucas-Dias, J. (2011). Phase locked matrix factorization. In *Proc. of the EUSIPCO Conference*.

Baker, S. N., Chiu, M., and Fetz, E. E. (2006). Afferent encoding of central oscillations in the monkey arm. *Journal of neurophysiology*, 95(6):3904–3910.

Cordivari, C., Lees, A. J., Misra, V. P., and Brown, P. (2002). Emg–emg coherence in writer's cramp. *Movement disorders*, 17(5):1011–1016.

de Carvalho, M. (2012). Testing upper motor neuron function in amyotrophic lateral sclerosis: the most difficult task of neurophysiology. *Brain*, 135(9):2581–2582.

Farmer, S. F., Gibbs, J., Halliday, D. M., Harrison, L. M., James, L. M., Mayston, M. J., and Stephens, J. A. (2007). Changes in emg coherence between long and short thumb abductor muscles during human development. *The Journal of physiology*, 579(2):389–402.

Fisher, K. M., Zaaimi, B., Williams, T. L., Baker, S. N., and Baker, M. R. (2012). Beta-band intermuscular coherence: a novel biomarker of upper motor neuron dysfunction in motor neuron disease. *Brain*, 135(9):2849–2864.

Grosse, P., Cassidy, M., Brown, P., et al. (2002). Eeg-emg, meg-emg and emg-emg frequency analysis: physiological principles and clinical applications. *Clinical neurophysiology: official journal of the International Federation of Clinical Neurophysiology*, 113(10):1523.

Grosse, P., Edwards, M., Tijssen, M., Schrag, A., Lees, A. J., Bhatia, K., and Brown, P. (2004). Patterns of emg–emg coherence in limb dystonia. *Movement disorders*, 19(7):758–769.

Halliday, D. M., Conway, B. A., Farmer, S. F., and Rosenberg, J. R. (1998). Using electroencephalography to study functional coupling between cortical activity and electromyograms during voluntary contractions in humans. *Neuroscience letters*, 241(1):5–8.

Hansen, N. L., Conway, B. A., Halliday, D. M., Hansen, S., Pyndt, H. S., Biering-Sørensen, F., and Nielsen, J. B. (2005). Reduction of common synaptic drive to ankle dorsiflexor motoneurons during walking in patients with spinal cord lesion. *Journal of neurophysiology*, 94(2):934–942.

Jackson, A., Spinks, R., Freeman, T., Wolpert, D., and Lemon, R. (2004). Rhythm generation in monkey motor cortex explored using pyramidal tract stimulation. *The Journal of Physiology*, 541(3):685–699.

Kiernan, M. C., Vucic, S., Cheah, B. C., Turner, M. R., Eisen, A., Hardiman, O., Burrell, J. R., and Zoing, M. C. (2011). Amyotrophic lateral sclerosis. *The Lancet*, 377(9769):942–955.

Klimesch, W., Freunberger, R., Sauseng, P., and Gruber, W. (2008). A short review of slow phase synchronization and memory: evidence for control processes in different memory systems? *Brain research*, 1235:31–44.

Marsden, J., Ashby, P., Limousin-Dowsey, P., Rothwell, J., and Brown, P. (2000). Coherence between cerebellar thalamus, cortex and muscle in man cerebellar thalamus interactions. *Brain*, 123(7):1459–1470.

Nishimura, Y., Morichika, Y., and Isa, T. (2009). A subcortical oscillatory network contributes to recovery of hand dexterity after spinal cord injury. *Brain*, 132(3):709–721.